Report to DRBC on concentrations of nutrients and chlorophyll *a* and rates of respiration and primary production in samples from the Delaware River collected in May and July 2019

Thomas R. Fisher
Professor

Anne B. Gustafson
Senior Faculty Research Assistant

Horn Point Laboratory
Center for Environmental Science
University of Maryland
2020 Horn Point Road
Cambridge MD 21613

Introduction

In December 2012, the Delaware River Basin Commission (DRBC) convened a Modeling Expert Panel to initiate work on development of an eutrophication model of the Delaware Estuary. This model was envisioned as a needed step toward the development of updated water quality criteria for dissolved oxygen and numeric nutrient criteria for the estuary, as described in DRBC's Nutrient Criteria Development Plan (http://www.nj.gov/drbc/library/documents/nutrients/del-river-estuary_nutrient-plan_dec2013.pdf). The Expert Panel reviewed existing information with DRBC and recommended among other activities the collection of new primary productivity and respiration data in the Delaware River and Estuary. In 2014 we measured nutrients, oxygen, water column extinction coefficients, respiration, and primary productivity in the lower Delaware estuary (RM 0 – 40) as an initial response to the Expert Panel recommendation (Fisher and Gustafson 2015). In 2018 we provided a similar set of data for the Delaware River stations at RM 71-131 in May and July, and here we provide a second set of measurements for the Delaware River stations RM 71-131 collected in May and July 2019. In the Discussion section of this report we make some comparisons between the three sets of data from the upper and lower portions of the Delaware River and Estuary.

As in previous years, sampling was conducted on two dates in 2019. On May 20, 2019 and July 16, 2019, DRBC staff collected surface and bottom water samples along five lateral transects at River Miles 71, 86, 101, 116, and 131. Samples were collected at three sites on each lateral transect (main channel, left of channel, and right of channel). At transects where the main channel ran along the shoreline, samples were collected at only two sites (RM 86-R was not sampled in May 2019 due to windy conditions). In May 2019 a total of 12 sites were sampled, and 24 water samples (surface and bottom) were collected (see Table 1, Fig. 1). In July 2019, a total of 13 sites were sampled, and 26 water samples were collected (see Table 1, Fig. 1). At each of the sites, surface and bottom measurements of salinity, temperature, and dissolved oxygen (DO) were made, and DRBC also measured photosynthetically active

radiation (PAR) above the water and at one meter below the water surface to provide data to estimate

the PAR extinction coefficient (k, m^{-1}, see Methods below). Water samples were picked up by HPL

personnel on the day of collection, transported to HPL in dark coolers, and stored at an appropriate

temperature and light regime overnight before measurements began the next day.

Methods

Field data were collected by DRBC personnel *in situ*. Salinity, temperature, and dissolved oxygen (DO) data at the surface and bottom were obtained using a Measurement Specialties Eureka 3 water quality meter. Light extinction measurements were made using a LiCor LI-1400 data logger connected to a LI-190 surface PAR sensor and a LI-192 underwater sensor. Both sensors had been calibrated by LiCor on January 19, 2018. At each station, surface irradiance (I_O, $\mu E\ m^{-2}\ s^{-1}$) was measured simultaneously with irradiance at a depth z = 1 m (I_Z, $\mu E\ m^{-2}\ s^{-1}$). The light extinction coefficient in the water column (k, m^{-1}) was estimated from these data as follows:

$$k = \ln(I_O/I_Z)/z = \ln(I_O/I_Z) \qquad\qquad \text{eq. 1}$$

for z = 1 m. These measurements were made *in situ* on the vessel when the water samples were taken for subsequent analysis of nutrients, respiration, and primary production in our laboratory.

Water samples were collected at 12-13 stations (12-13 surface samples, 12-13 bottom samples) as described in the introduction by DRBC personnel on an 18-foot jon boat. Collected water samples were maintained at ambient water temperature at 60% light (surface samples) or in darkness (bottom water samples) while on the vessel. At the dock the samples were transferred late in the day to coolers to maintain water temperature as much as possible, and the samples were then driven to HPL on the day of sampling. Within 2.5 h of the ship's arrival at the dock, the samples were transferred to a BOD box at the Horn Point Laboratory (HPL) maintained at 16.3°C in May and 25.7°C in July to approximate the median bay temperatures observed (range = 15.4-17.8°C in May, 25.6-29.9°C in July). Lights within the BOD box provided ~100 $\mu E\ m^{-2}\ s^{-1}$ of PAR on the appropriate day/night cycle for the month. Bottom samples were wrapped in black bags within the BOD box to maintain darkness and ambient temperature. On the morning following sample collection, aliquots of the samples were placed in incubation bottles for measurements of respiration (all samples) and ^{14}C-based primary production (surface samples only). Details are provided below.

Samples for nutrients (NH_4, NO_2+NO_3, and PO_4, µM = µmoles L^{-1} = mmoles m^{-3}) and chlorophyll a (chla, µg L^{-1} = mg m^{-3}) analyses were filtered following the start of the incubations. N and P concentrations can be converted to mg/L using 1 µmole N L^{-1} = 0.014 mg N L^{-1} and 1 µmole P L^{-1} = 0.031 mg P L^{-1}. Filtered samples were frozen at -5°C and analyzed for nutrients within one month by automated colorimetry on a Technicon 2 AutoAnalyzer in the HPL Analytical Services Laboratory following the protocols of Lane et al (2000). The protocols followed EPA standard methods 350.1 for NH_4^+ (ammonium), 353.2 for $NO_3^- + NO_2^-$, (nitrate and nitrite), and 365.1 for PO_4^{-3} (soluble reactive phosphate). Filters for chla (chlorophyll *a*) analysis were frozen and stored at -80°C until analysis by fluorometry on a Turner Designs model 10-AU in the HPL Analytical Services Laboratory, generally within 2 months. The chla protocol followed the EPA 445.0 standard method.

Respiration was measured as the difference in oxygen concentrations (O_2, mg O_2 L^{-1}) between an initial measurement and a final measurement after a dark incubation of ~24 hours. Initial and final samples were put into quadruplicate, 12 ml, darkened, Exetainer tubes with septa caps (Labco, Inc.) to exclude air contact. The initial samples were processed in sequence within two hours as described below, and the remaining bottles were transferred to an incubator floating in the HPL boat basin subject to Choptank River temperatures and damped wave action. Final samples were returned to the lab ~24 hours later and were also analyzed in sequence for O_2 on the same day. All of the respiration samples were analyzed for O_2 by Membrane Inlet Mass Spectrometry (MIMS, Kana et al. 1994) with a precision of <0.5%. The first replicate of each set of four for each sample was used to condition the MIMS, and the remaining three were averaged for DO. MIMS simultaneously measures dissolved N_2, O_2, and Ar with high precision, and the ratios of N_2 and O_2 to Ar can be used to assess saturation relative to air equilibrium. The difference between the initial and final DO (DO_i, DO_f, mg O_2 L^{-1}) was used to calculate Respiration (R, mg O_2 L^{-1} d^{-1}, equivalent to g O_2 m^{-3} d^{-1}), as follows:

$$R = (DO_f - DO_i)/\Delta t \qquad\qquad\qquad \text{eq. 2}$$

where Δt = time in days calculated from the average time of initial and final analyses for each station. Since DO_i was greater than DO_f, with the exceptions noted below, R was negative, representing net consumption of O_2. For the exceptions at stations RM-131-LS, CS; RM 116 LS, there was an anomalous increase in O_2, and we have not used the respiration value from these surface stations in the analyses below. These were the first four samples measured for DO_i and DO_f, and we attribute the anomalous results to an initial drift in instrument calibration.

Primary production measurements were performed on the samples stored overnight in the BOD box maintained at an appropriate diel light regime (described above). Six aliquots of sample (148 ml) were transferred to rinsed, transparent, 150 ml bottles. We added 0.1 ml of a ^{14}C-$NaHCO_3$ solution (1 μCi/ml activity) to each bottle, capped each bottle, mixed thoroughly, and filtered one of the bottles immediately to correct for particulate contaminants in the stock and ^{14}C sorption on particulates in the original water sample. The other five bottles were transferred into screened bags of varying thicknesses to attenuate the light to 60%, 32%, 15%, 7.5%, and 3.0% of surface Photosynthetically Active Radiation (PAR, 400-700 nm, E m^{-2} d^{-1}), which was monitored on the roof of HPL and calculated as described in Fisher et al. (2003). The bottles in their screens were then quickly transferred to the floating incubator described above, and incubated for ~24 hours, when they were returned to the laboratory for filtration. The incubation period was terminated when the samples had received the equivalent of an average day of PAR for May or July (Fisher et al. 2003), adjusting for overcast or very sunny days. Following filtration on 25 mm GFF filters at <200 mm Hg vacuum, all filters (including the edges under the filter funnel) were rinsed with filtered sample water from the original sample to remove dissolved ^{14}C and then transferred to 7 ml scintillation vials with 7 ml of Ecoscint A fluor. Total ^{14}C activity (TA, dpm/ml) was measured using the addition of 0.1 ml of the ^{14}C stock to Ecoscint A fluor. All scintillation vials were allowed to sit for 24 hours in the Packard Tricarb model 2200CA liquid scintillation counter to eliminate auto-fluorescence from ambient light, and then counted to 1% accuracy. Total CO_2 (TCO_2 = sum of CO_2, H_2CO_3,

HCO_3^-, and CO_3^{-2}) was calculated using the relationship of carbonate alkalinity to salinity reported for Delaware Bay by Sharp (2013). Primary production at simulated depth z (P_z, mg C L^{-1} d^{-1} = g C m^{-3} d^{-1}) was calculated as follows:

$$P_z = 1.05 * TCO_2 * (DPM_f – DPM_i) / (TA * \Delta t) \qquad\qquad\qquad \text{eq. 3}$$

where 1.05 corrects for the isotopic discrimination for $^{14}C\text{-}CO_2$ uptake compared to $^{12}C\text{-}CO_2$ uptake, DPM_f and DPM_i are the ^{14}C activity of the final and initial samples for each light level, and Δt is the time interval of the incubation in days (approximately 1 day).

In general, we adhered to the protocols of Sharp et al. (2009) and Sharp (2013) for primary production measurements to maintain continuity with existing primary production datasets. Deviations from Sharp's protocols included: (1) lower ^{14}C activity added to our samples (0.1 µCi in 150 ml bottles vs 1 µCi in 80 ml bottles by Sharp), and (2) our attenuation screens were virtually identical to those used by Sharp, but we used a 3% compared to a 1.5% PAR level for the highest light attenuation (lowest light level). Neither of these deviations should have any significant effect on the rates of primary production at a given depth (P_z, g C m^{-3} d^{-1}) or integrated primary productivity (P, g C m^{-2} d^{-1}) reported here for comparison with Sharp's previous datasets.

We used the hyperbolic tangent model of Jassby and Platt (1976) to evaluate the effect of PAR on rates of primary production at any depth z (m) as (P_z):

$$P_z = P_m * \tanh(x) \qquad\qquad\qquad\qquad\qquad \text{eq. 4}$$

where P_m is the maximum, light-saturated primary production (g C m^{-3} d^{-1}). P_m is the asymptote as P_z approaches saturation, and x is a composite parameter defined as follows:

$$x = \alpha * PAR / P_m \qquad\qquad\qquad\qquad\qquad \text{eq. 5}$$

where α is the light-dependent primary productivity parameter (initial slope of P_z vs PAR with units of g C m^{-3} $(E\ m^{-2})^{-1}$. Values of P_z for each station at varying PAR within the attenuating screens were fit with the hyperbolic tangent function to obtain α and P_m. This equation is equivalent to models 1 (linear) and

2 (hyperbolic saturation) used by Sharp (2013). In the dataset reported for May and July 2014 in Delaware Bay (Fisher and Gustafson 2015) and for May and July 2018 in the Delaware River (Fisher and Gustafson 2018), we saw no evidence of light inhibition (Sharp's model 3).

For ease of fitting the hyperbolic tangent (tanh) function to the P_z vs PAR data in SigmaPlot v12.5, we used the following transformation:

$$\tanh(x) = (e^{2x} - 1)/(e^{2x} + 1) \qquad \text{eq. 6}$$

which was obtained from:

http://www.roperld.com/science/Mathematics/HyperbolicTangentWorld.htm

In our application, we used the following formulation:

$$P_z = P_m * (e^{2*\alpha*PAR/Pm} - 1)/(e^{2*\alpha*PAR/Pm} + 1) \qquad \text{eq.7}$$

where e is the exponential function, and all other parameters are described above. The hyperbolic tangent function fit the data well ($r^2 > 0.86$ see Fig. 2A, Tables 3A and 3B), and we were able to estimate α, the light-dependent primary production parameter (g C m^{-3} (E m^{-2})$^{-1}$) for every station that was sampled. However, for all but two of the May 2019 samples (RM 101-LS and RM 71-LS) and for six of the July 2018 samples in the upper transect of the river, the relationship between P and PAR was essentially linear (Sharp's model 1), which enabled us to obtain α, but which prevented us from estimating P_m, the light-saturated primary production parameter (P_m, g C m^{-3} h^{-1}), which is independent of PAR. For consistency, we used eq. 7 to calculate α for all stations, but for 11 May stations and 6 July stations, P_m was indeterminate.

We estimated integrated water column primary productivity (P, g C m^{-2} d^{-1}) using the measured water column extinction coefficient (k, m^{-1}, eq. 1) and the observed values of C fixation (P_z) at the fixed light depths of 3-60%. Using k, we converted the light depth into water depth (z, m):

$$z = \ln(I_O/I_z)/k \qquad \text{eq. 8}$$

where I_O is the total PAR (E m^{-2} d^{-1}) during the incubations and I_z is the calculated irradiance at the light

depth ($E\ m^{-2}\ d^{-1}$) based on the extinction coefficient (k) of each station. I_O was obtained using a LiCor-190 surface probe on the roof of a building at Horn Point Laboratory attached to a LI-1000 data logger (see Fisher et al. 2003) integrated at hourly intervals (May 2019: 41 $E\ m^{-2}\ d^{-1}$, July 2019: 48 $E\ m^{-2}\ d^{-1}$). We extrapolated the observed volumetric C fixation rate at each depth to the midpoint between each depth above and below (Δz, m), except that the production at 60% light was extrapolated to the surface and the production at 3% light was extrapolated to one additional depth increment below the estimated value. P was estimated as:

$$P = \Sigma\ (Pz*\Delta z) \qquad\qquad\qquad\qquad\qquad\qquad\qquad\text{eq. 9}$$

See Fig. 6B for an example.

All statistical analyses were done in SigmaPlot v12.5 and Excel 2010. The significance level for statistical tests was set at $0.05 < p < 0.10$ (marginally significant), $0.01 < p < 0.05$ (significant) or $p < 0.01$ (highly significant), unless otherwise noted. When terms with errors were combined in a formula, propagation of error for the final result was based on error in the individual components using the standard error propagation formulas in Bevington (1969), assuming no error covariance. Parametric statistical comparisons and tests were done if the data were normally distributed; otherwise an equivalent non-parametric test was used.

Results and Discussion

Nutrients

Concentrations of dissolved nutrients were moderately high on both cruises in 2019 (Tables 1 and 2). Ammonium (NH_4^+) had the lowest concentrations of N, ranging over 0.7 – 11.7 µM on both cruises, averaging 3.6 ± 0.7 in May and somewhat lower in July (2.4 ± 0.4, $p<0.05$). There were no significant differences ($p>0.10$) between surface and bottom water NH_4^+ at all stations on each cruise, although there was some lateral variability across the river for NH_4^+ and phosphate (PO_4^{-3}, Fig. 2). Nitrate (NO_3^-) was more abundant than ammonium, ranging over 53 - 122 µM on both cruises and averaging 62 ± 3 in May and significantly higher in July (97 ± 4, $p<0.05$). As for NH_4^+, there were no significant differences ($p>0.10$) in NO_3^- concentrations between surface and bottom waters at each station but little lateral variability. Phosphate (PO_4^{-3}) had the lowest concentrations of the three major nutrients, ranging over 0.45- 2.09 µM on both cruises and averaging 0.66 ± 0.03 in May and marginally significantly higher in July (1.32 ± 0.05, $p=0.07$). Comparing the seasonal differences in the two cruises, NO_3^- and PO_4^{-3} were both higher in the July cruise, and the ranges of NH_4^+ overlapped in both months.

The dissolved inorganic N (DIN = NH_4^+ + NO_3^-) and PO_4^{-3} concentrations reported in Tables 1 and 2 are considered saturating for phytoplankton growth in estuaries (Fisher et al. 1995, 1999). For all stations, both dissolved inorganic N (DIN = NO_3^- + NH_4^+) and PO_4^{-3} were sufficiently abundant that it is likely that light and not nutrients were limiting phytoplankton growth rates. As shown below, there was little evidence for vertical stratification, and deep mixing occurred in these upper Delaware River stations with moderate to high turbidity.

In our 2014 report on the lower Delaware Bay, we explored nutrient concentrations across the salinity gradient to illustrate net ecosystem processing. However, we are unable to explore the mixing behavior of nutrients in this report because all of the stations were fresh or nearly so. Salinities ranged over 0.09-0.21 in both May and July 2019, with <0.003 salinity differences between top and bottom

samples. Temperatures ranged over 15-18°C in May and 26-28°C in July, with <0.5°C temperature differences between all surface and bottom samples (Tables 1 and 2). Therefore, there was no evidence of significant surface to bottom differences in density or stratification at any of the stations.

To show the longitudinal distributions of nutrients, we have plotted them as a function of river mile (RM, Fig. 2). For the May cruise, the spatial distribution of NO_3^- between RM 70 to 131 (top panel) exhibited a maximum of ~90 μM at RM 71-86 near Wilmington DE, decreasing upstream to ~60 μM towards Trenton. In July 2019, nitrate concentrations were systematically higher than in May, with a July maximum of ~120 μM at Wilmington and a secondary maximum at Trenton of ~100 μM. Ammonium in May had a nearly flat spatial distribution with a small maximum concentration of ~3 μM at RM101 near Philadelphia and Camden. In contrast, NH_4^+ in July was low, ~1 μM at Philadelphia/Camden and in the lower river, increasing to 3-5 μM in the upper river towards Trenton. Although we have no rate data for confirmation, this pattern is consistent with an excess of NH_4^+ inputs from land or regeneration of NH_4^+ relative to nitrification within the water column and sediments of the upper river in July, leading to a small accumulation of NH_4^+ in the water column in July. We saw a similar pattern in May 2018 in our previous report, but the pattern in 2019 occurred in July. The distribution of PO_4^{-3} along the river was relatively flat in both months, and PO_4^{-3} was systematically higher in July, as also seen in 2018, with a small maximum (~2 μM) in the upper river in July 2019.

Chlorophyll *a*

Phytoplankton biomass, as indicated by chlorophyll *a* concentrations (chla), ranged from 1 - 58 μg L^{-1} along RM 71-131 of the river during both May and July 2019 (Tables 1-2, Figs. 3A-B, middle panels). In May 2019 there was little systematic difference between surface and bottom chla, particularly in the upper river at RM 101-131, and chlorophyll *a* also increased greatly to bloom proportions (40-60 μg L^{-1}) between RM86 (Chester) and RM 71 (Wilmington). These high values of

chlorophyll a observed in May 2019 in the Delaware River near Wilmington are indicative of eutrophic conditions considerably greater than the chlorophyll a criterion of 15 µg L^{-1} derived for Chesapeake Bay based on a variety of associated water quality criteria (Harding et al. 2014). In July 2019 chlorophyll a was lower in surface waters, but chlorophyll a concentrations in bottom waters were significantly higher than in surface waters at RM 71 (Chester) to RM 101 (Philadelphia).

Because phytoplankton consume nutrients as they increase in biomass, chlorophyll a is often inversely related to concentrations of NO_3^- and PO_4^{-3}, as was observed on the two cruises in 2014 (Fisher and Gustafson 2015). However, on the two cruises in 2019 in the Delaware River, there were few significant correlations between nutrients and chla (Fig. 4). Chlorophyll a concentrations were **positively** correlated with concentrations of NO_3^- in May 2019 (r^2 = 0.93, p<0.01), but there were no significant relationships between chlorophyll a and PO_4^{-3}. The lack of inverse relationships between nutrients and chlorophyll a suggests that phytoplankton uptake does not have an important effect on nutrient concentrations in the river, leaving nutrient inputs as the dominant control of nutrient concentrations.

Dissolved Oxygen

The distributions of dissolved O_2 (DO), chlorophyll a (chla), and respiration (R) along the river are shown for May (Fig. 3A) and July (Fig. 3B). Consistent with the lack of stratification in the Delaware River, there were no significant vertical differences in DO in May, although there were significantly lower DO values in bottom water at 3 of the 5 stations in July. In May, DO was close to air saturation at 17°C, with ~10% under-saturation at RM 116 between Wilmington and Philadelphia. In the July DO data at temperatures of ~27°C, there was 10-30% under-saturation of O_2 throughout most of the river (except at Trenton).

<u>Respiration</u>

Respiration (R, g O_2 m^{-3} d^{-1}) ranged over -0.02 to -0.77 in both May and July 2019 along RM 71-131 (Tables 1-2, Fig. 3A, B). In May R was significantly higher in bottom waters compared to surface waters of the Delaware River, whereas in July 2019 there were no consistent differences between respiration in surface and bottom waters. There were also no significant differences between R at the RM stations between May and July, with both sets of data ranging over -0.02 to -0.77 g O_2 m^{-3} d^{-1}, despite the large temperature difference (17.0 vs 26.5°C). This overlap of respiration rates was also observed for the May and July data of 2014 for the lower Delaware Bay (Fisher and Gustafson 2015) and in the upper river in May and July 2018 (Fisher and Gustafson 2019).

Along the Delaware River, respiration was distributed in a spatial pattern similar to that of chlorophyll *a*. The relationship between respiration and chlorophyll a can be seen in Fig. 5. There were significant correlations between R and chla in both May and July (r^2 = 0.53 -0.35, respectively, Fig. 5), with significantly higher respiration in bottom waters in May 2019. This suggests that much of the respiration was by phytoplankton or by heterotrophic organisms associated with the phytoplankton in the river. The relationship between respiration and chlorophyll *a* in May is primarily driven by the very high chla and respiration values observed at station RM71. In May and July 2014 and May and July 2018, we also observed strong correlations between respiration and chla in the lower Delaware Bay and upper river stations, respectively.

Because respiration was generally related to chlorophyll *a*, we normalized each value of respiration to the observed chlorophyll *a* at each station (Tables 1, 2). This resulted in a community respiration value per unit chlorophyll *a* of phytoplankton (R^B, g O_2 mg chla^{-1} h^{-1}). In our 2014 report on respiration in the lower Delaware Bay, we found that this approach minimized variance in respiration rates; however, in the 2018 data this was not the case. In May 2019 the %se/mean for R was 27%, a value larger than for R^b (19%); however, for July 2019, the values for R and R^b were closer (14% and 16%,

respectively). It appears that R^b does not consistently reduce the variance as a respiration parameter compared to R. However, for comparison with the 2014 lower Bay data, we have retained the computation of R^B in the 2018 and 2019 data for the Delaware River.

Primary Production

There was a strong light dependence of C fixation at a depth z (P_Z, primary production) in the May and July datasets (see examples in Fig. 6A, B). The hyperbolic tangent provided easy parameter estimation for α (g C m^{-3} (E m^{-2})$^{-1}$), the light-dependent increase in C fixation with increasing PAR, and for P_m (g C m^{-3} d^{-1}), the light-independent, maximum rate of C fixation (Tables 3A and B, Fig. 6A lower panel). Only 2 of the 12 river stations were fit well by the hyperbolic tangent function in May 2019, but 7 of the thirteen river stations were hyperbolic in July 2019. The other stations exhibited essentially a linear relationship between C fixation and PAR (Sharp type 1 P vs PAR curves, upper panel of Fig. 6A). At these stations, we obtained good estimates of α, the light-dependent parameter, but it was not possible to estimate P_m because P_Z increased up to the highest PAR available on the incubation day (41 E m^{-2} d^{-1}, in May and 48 E m^{-2} d^{-1} in July, or about 93% of the average PAR in May and 101% in July (Fisher et al. 2003) due to partly cloudy conditions during the incubations.

The photosynthetic parameters α and P_m (Tables 3A and B) were more variable in May than in July 2019. The light-dependent parameter α varied over 1-2 orders of magnitude in May (0.003-0.208 g C m^{-3} (E m^{-2})$^{-1}$, with an average ± se = 0.035 ± 0.017 (Table 3A). In contrast, in July 2019 α varied only by a factor of ~5 (0.008-0.038 g C m^{-3} (E m^{-2})$^{-1}$, with an average ± se = 0.020 ± 0.003, Table 3B). A Wilcoxon signed-rank test indicated that the July values of α were not significantly different than the May values at paired stations ($p>0.10$). The light saturated rate of photosynthesis P_m ranged over 0.08-0.66 g C m^{-3} d^{-1} in May, with an average of 0.37 ± 0.29 (n=2, Table 3A); in July the P_m values were about twice as high as in May (range = 0.54 – 0.92, average ± se = 0. 70 ± 0.04, n=7, Table 3B). A paired t test indicated no

significant differences between the two sets of values of P_m at paired stations during May and July due to insufficient degrees of freedom.

The photosynthetic parameters α and P_m were significantly correlated. Using data from both May and July, P_m was related to α by an hyperbolic tangent function (Fig. 7). Because of the scatter in the data, the use of an hyperbolic function in Fig. 7 is somewhat arbitrary, and the data can be fit well by linear, exponential, and hyperbolic functions. However, despite the statistical uncertainty, a hyperbolic function is consistent with a physiological upper limit to P_m as α increases, and we also observed a clear hyperbolic relationship between P_m and α in the 2014 and 2018 data (Fisher and Gustafson 2015, 2019). A linear fit may seem to be the simplest relationship, but it yields a positive intercept on the Y axis, a physiologically impossible situation that would suggest a P_m with zero α.

Both α and P_m were influenced by chlorophyll *a* concentrations (Fig. 8). There was a significant linear correlation between α and chlorophyll *a* over a broad range of values in May 2019 (r^2 = 0.90, p<0.01), but in July α was negatively related to chlorophyll *a* over a narrow range of chlorophyll *a* (Fig. 8, upper panel). This relationship between α and chlorophyll a in July is difficult to assess, but could be spurious due to the narrow range of river chlorophyll *a* observed in July. P_m showed a somewhat similar relationship with chlorophyll *a*: a linear relationship between P_m and chlorophyll *a* in May, but not in July (Fig. 8, lower panel). Although the linear relationship between P_m and chlorophyll *a* in May is similar to that between α and chlorophyll *a* in May (Fig. 8, upper panel), there were only two stations in May 2019 with a measurable P_m, with insufficient degrees of freedom to evaluate the relationship statistically.

As we did for the respiration data, we have attempted to remove the effect of phytoplankton biomass (chlorophyll *a*) on the photosynthetic parameters. We normalized α and P_m with the observed chlorophyll *a* to create the biomass-specific, light-dependent, photosynthetic parameter α^b with units of g C (E m^{-2})$^{-1}$ (mg chla)$^{-1}$ and the biomass-specific, light-independent, photosynthetic parameter $P_m{}^b$ with units of g C (mg chla)$^{-1}$ d^{-1} (Tables 3A, B). These biomass-specific parameters are useful for comparison

with measurements of primary production in other Delaware Bay datasets and in other environments.

There were some effects of the light extinction coefficient k (m^{-1}) on the photosynthetic parameters α, α^b, P_m, and P_m^b. In Fig. 9A, we have plotted both α and α^b as a function of k for May 2019. There was a significant exponential relationship ($r^2 = 0.90$, $p<0.01$) between α and k in the upper panel, implying that the light sensitive uptake of CO_2 (α) is adapting to turbid conditions (high k); similar results were shown in the 2018 dataset (Fisher and Gustafson 2019). When we removed the effect of chlorophyll *a* on α by plotting α^b versus k in the lower panel, there appeared to be an inverse exponential relationship. However, there was too much scatter in the data, and the fit of the curve was not significant ($p=0.15$). In May 2018, we also found a negative, exponential relationship between P_m^b and k which was significant ($r^2=0.43$, $p<0.05$; Fig. 9B, lower panel of Fisher and Gustafson 2019).

In July 2019 we found weaker relationships between α, α^b, and k. There was a weak inverse relationship between α and k ($r^2 = 0.40$, $p<0.05$, upper panel, Fig. 9B), which implies that the light dependent rate of CO_2 uptake was lower in more turbid areas of the Delaware River. This is the opposite of what we observed in the previous May and suggests no light adaptation in July. There was no significant relationship between the biomass-normalized, light-dependent rate of C fixation (α^b) and k, the extinction coefficient in the water column (Fig. 9B, lower panel).

In May 2019 we measured only two examples of the light-saturated rate of photosynthesis (P_m). For this reason we have combined the values of P_m for May and July to examine their relationship with the extinction coefficient k. The upper panel of Fig. 9C shows a marginally significant, positive relationship between P_m and k ($r^2= 0.48$, $p = 0.054$). Although this relationship implies light adaptation (higher Pm in more turbid waters), the relationship is totally dependent on the two points from May 2019. Likewise there is a non-significant relationship between P_m^b and k (lower panel Fig. 9C). Both of these relationships in Fig. 9C are probably spurious.

Depth-integrated primary productivity (P, g C m^{-2} d^{-1}) in 2019 ranged over almost an order of

magnitude (0.1-0.7 g C m^{-2} d^{-1}, Fig. 10). There was no significant difference between values of P in May

and July 2019 (Tables 3A, B), and these P values in 2019 occurred in the lowest range of P values

measured in Delaware Bay in 2014 (0.4-6 gC m^{-2} d^{-1}; Fisher and Gustafson 2015). As in 2018, the highest

values of P in 2019 occurred at the most downstream stations RM86 to RM71 in May (Table 3A),

whereas P was more evenly distributed in July with the highest values in the upper river at stations

RM116 to RM 86 (Table 3B). Because P was computed using α and P$_m$, the effects of chla and k on P

were similar (Fig. 10). In the upper panel of Fig. 10 there is a positive, exponential relationship between

P and chlorophyll *a* in the combined data from May and July 2019. In contrast, in the lower panel of Fig.

10 there was no significant relationship between P in either the individual months or combined

datasets. As in the 2014 (lower Delaware Bay) and 2018 (Delaware River) data, the relationships in Figs.

6-10 potentially provide an empirical basis for estimating the photosynthetic parameters α, P$_m$, and P

using relatively simple field measurements of chlorophyll *a*, k, and PAR.

Conclusions and Synthesis

It is clear that the Delaware River and Bay are nutrient-enriched from its upstream basin. Nitrate, in particular, is quite high in the freshwater end-member (100-120 µM, Fig. 2), similar to the range found in 2014 in mixing curves (100-120 µM, Fisher and Gustafson 2015) and in the Delaware River in 2018 (Fisher and Gustafson 2019). These river values are essentially equivalent to concentrations in the Susquehanna River that largely drive eutrophication and hypoxia in the mainstem of Chesapeake Bay (Fisher et al. 1988, Glibert et al. 1995, Kemp et al. 2005). Nutrient concentrations within the Delaware River and Estuary are typically above levels considered saturating for phytoplankton growth, and chlorophyll *a* concentrations generally declined upriver but were often 20-30 mg m^{-3} in the lower river upstream of the turbidity maximum, which is typically near Chester (between RM71 and RM86). These chlorophyll a values greater than 15 mg m^{-3} are associated with poor water quality and hypoxia in Chesapeake Bay (Harding et al. 2014). There are also significant correlations between chlorophyll *a*, nutrients, respiration, and primary production (Figs. 4, 5, 8, 10) indicating linkages between the water column parameters measured in this study.

Rates of both respiration and primary productivity are moderately high in the Delaware River. Why then do we observe so little hypoxia in Delaware Bay compared with Chesapeake Bay? There is some hypoxia, of course, in the Delaware River, particularly in July 2019 (Figs. 3A, B). Both surface and bottom waters were ~10-30% undersaturated in O_2 compared to atmospheric equilibrium, particularly downstream of Trenton to Wilmington (Figs. 3A, B). This under-saturation of O_2 indicates regions of net respiration and consumption of organic matter (net heterotrophy) in these river sections. However, compared to the near anoxia of the Chesapeake Bay mainstem and some tributaries in summer (e.g., Hagy et al. 2004), the impact of the nutrients on Delaware Bay is relatively small in terms of dissolved oxygen.

The difference between these two estuarine systems lies in their physics. Chesapeake Bay was

over-deepened during the last glacial maximum and is still filling in the former Susquehanna River valley that we now call Chesapeake Bay. Delaware Bay has access to larger sand supplies which have filled in the former Delaware River valley now known as the lower Delaware estuary. Furthermore, the lower Delaware estuary is shallow and funnel-shaped, amplifying the tidal amplitudes towards the freshwater end. This results in enhanced flushing and mixing energy compared to Chesapeake Bay, which widens and deepens from its mouth, resulting in damped tides, less flushing, and low mixing energy in its strongly stratified mid-section. As a result, Chesapeake Bay is density-stratified for much of the year, cutting off the supply of atmospheric O_2 from bottom waters and enhancing hypoxia. In contrast, shallow Delaware Bay is mixed by big tides and is frequently unstratified by density, allowing ventilation of biologically driven oxygen deficits and surpluses in low and high salinity waters, respectively, in both surface and bottom waters, despite the development of relatively high values of phytoplankton biomass. The contrast between these two adjacent estuarine systems is quite striking.

Is the water quality in Delaware Bay cause for concern? In the two time periods examined here (May and July 2019), there were moderate deviations from O_2 atmospheric equilibrium in surface or bottom waters of the upper river, indicating minimal impact on dissolved O_2. We reported similar results from the 2014 and 2018 data (Fisher and Gustafson 2015, 2018). Much of the nutrients appear to be assimilated in the lower bay where the subsequent organic matter is likely subject to dispersal on the continental shelf. Although chlorophyll *a* concentrations at the upper stations of the Delaware River in 2019 were high (10-60 mg m^{-3}), in May 2014 chlorophyll a concentrations exceeded 100 mg m^{-3} in the Delaware Estuary (Fisher and Gustafson 2015). Values of that magnitude are often associated with harmful algal blooms, which can have significant impacts on fisheries, recreational activities, and human health (Harding et al. 2014). Reducing nutrient inputs in the upper estuary and in the river basin would reduce the potential for harmful algal blooms in the lower bay.

References

Bevington, P. R. 1969. Data Reduction and Error Analysis for the Physical Sciences. McGraw-Hill Book Co., NY, 336 pps.

Colt, J. 1984. Computation of dissolved gas concentrations in water as functions of temperature, salinity, and pressure. Amer. Fish. Soc. Spec. Pub. 14

Fisher, T. R., L. W. Harding, D. W. Stanley, and L. G. Ward. 1988. Phytoplankton, nutrients, and turbidity in the Chesapeake, Delaware, and Hudson River estuaries. Est. Coastal Shelf Sci. 27: 61-93

Fisher, T. R., J. M. Melack, J. Grobbellar, and R. W. Howarth. 1995. Nutrient limitation of phytoplankton and eutrophication of estuarine and marine waters. pps. 301-322 IN: H. Tiessen (ed.) Phosphorus cycling in Terrestrial and Aquatic Ecosystems. SCOPE, Wiley.

Fisher, T. R., A. B. Gustafson, K. Sellner, R. Lacuture, L. W. Haas, R. Magnien, R. Karrh, and B. Michael. 1999. Spatial and temporal variation in resource limitation in Chesapeake Bay. Mar. Biol. 133: 763-778

Fisher, T. R., A. B. Gustafson, G. R. Radcliffe, K. L. Sundberg, and J. C. Stevenson. 2003. A long-term record of photosynthetically active radiation (PAR) and total solar energy at 38.6° N, 78.2° W. Estuaries 26: 1450-1460

Fisher, T. R. and A. B. Gustafson. 2015. Concentrations of nutrients and chlorophyll a, and rates of respiration and primary production in samples from Delaware Bay collected in May and July 2014. Rep. DRBC, May 2015

Glibert, P. M., D. J. Conley, T. R. Fisher, L. W. Harding, Jr., and T. C. Malone. 1995. Dynamics of the 1990 winter/spring bloom in Chesapeake Bay. Mar. Ecol. Prog. Ser. 122:27-43

Hagy, J. D., W. R. Boynton, C. W. Keefe, and K. V. Wood. 2004. Hypoxia in Chesapeake Bay, 1950-2001: long-term change in relation to nutrient loading and river flow. Estuaries 27: 634-658

Harding, Jr., L. W., R. A. Batiuk, T. R. Fisher, C. L. Gallegos, T. C. Malone, W. D. Miller, M. R. Mulholland, H. W. Paerl, and P. Tango. 2014. Scientific bases for numerical chlorophyll criteria in Chesapeake Bay. Estuaries and Coasts 37: 134-148

Jassby, A. D. and T. Platt 1976. Mathematical formulation of the relationship between photosynthesis and light for phytoplankton. Limnol. Oceanogr. 21: 540-547

Kana, T. M., C. Darkangelo, M. D. Hunt, J. B. Oldham, G. E. Bennett, and J. C. Cornwell. 1994. Membrane inlet mass spectrometer for rapid high-precision determination of N_2, O_2, and Ar in environmental water samples. Anal. Chem. 66:4166-4170

Kemp, W. M., W. R. Boynton, J. E. Adolf, D. F. Boesch, W. C. Boicourt, G. Brush, J. C. Cornwell, T. R. Fisher, P. M. Glibert, J. D. Hagy, L. W. Harding, E. D. Houde, D. G. Kimmel, W. D. Miller, R. I. E. Newell, M. R. Roman, E. M. Smith, J. C. Stevenson. 2005. Eutrophication of Chesapeake Bay: Historical trends and ecological interactions. Mar. Ecol. Prog. Ser. 303: 1-29

Lane, L., S. Rhoades, C. Thomas, and L. Van Heukelem. 2000. Standard Operating Procedures of the Analytical Services Laboratory of the Horn Point Laboratory, Center for Environmental Science, University of Maryland. Tech. Rep. No. TS-264-00

Sharp, J. H., K. Yoshiyama, A. E. Parker, M. C. Schwartz, S. E. Curless, A. Y. Beauregard, J. E. Ossolinkski, and A. R. Davis. 2009. A biogeochemical view of estuarine Eutrophication: seasonal and spatial trends and correlations in the Delaware Estuary. Estuaries and Coasts 32: 1023-1043

Sharp, J. H. 2013. Biogeochemical Methods Manual. School of Marine Science and Policy, College of Earth, Ocean, and Environment, University of Delaware.

Table 1. Data Summary for Delaware Bay (20 May 2019). Respiration numbers in red are positive values at two upper river stations that were anomalous and not included in the statistics or subsequent data analyses. No water samples were collected at station RM86-RS in May 2019.

Station	Salinity	Temp °C	mg O$_2$ L^{-1} DO	μM NH$_4$	NO$_3$	PO$_4$	Chla, mg m^{-3} ave	se	g O$_2$ m^{-3} d^{-1} respiration	se	g O$_2$ (mg Chla)$^{-1}$ d^{-1} R^B	se
RM131-LS top	0.10	17.2	9.62	2.96	59.2	0.78	2.75	0.07	0.189	0.019	0.069	0.102
RM131-CS top	0.09	16.9	9.75	0.94	53.9	0.50	1.84	0.11	-0.017	0.016	-0.009	0.908
RM131-RS top	0.09	17.0	9.75	1.26	53.7	0.48	2.05	0.06	0.016	0.026	0.008	1.672
RM116-LS top	0.09	16.2	9.56	2.10	54.3	0.51	2.55	0.03	-0.025	0.014	-0.010	0.574
RM116-CS top	0.09	16.3	9.61	2.13	54.3	0.51	2.12	0.01	0.013	0.019	0.006	1.524
RM116-RS top	0.10	16.4	9.58	2.89	56.6	0.61	2.39	0.04	0.074	0.018	0.031	0.251
RM101-CS top	0.09	16.0	9.41	3.52	54.4	0.64	2.47	0.03	-0.044	0.029	-0.018	0.661
RM101-LS top	0.09	16.0	9.36	2.44	54.3	0.57	2.46	0.04	-0.008	0.019	-0.003	2.354
RM86-LS top	0.10	15.6	9.20	11.30	60.8	0.79	4.22	0.02	-0.060	0.038	-0.014	0.640
RM86-CS top	0.10	15.9	9.30	10.10	62.8	0.85	3.29	0.01	-0.106	0.021	-0.032	0.199
RM86-RS top												
RM71-CS top	0.13	17.7	9.09	2.59	89.2	0.75	38.09	0.26	-0.258	0.013	-0.007	0.050
RM71-LS top	0.13	17.8	9.30	1.31	89.1	0.62	57.77	2.67	-0.464	0.024	-0.008	0.069
RM131-LB bottom	0.10	17.1	9.64	2.75	58.9	0.82	2.56	0.06	-0.161	0.016	-0.063	0.103
RM131-CB bottom	0.09	16.9	9.77	1.00	53.5	0.47	1.73	0.01	-0.092	0.014	-0.053	0.156
RM131-RB bottom	0.09	16.9	9.78	1.00	53.6	0.45	1.90	0.09	-0.168	0.007	-0.089	0.061
RM116-LB bottom	0.09	16.1	9.62	3.18	54.5	0.55	2.33	0.01	-0.158	0.025	-0.068	0.157
RM116-CB bottom	0.09	16.2	9.68	3.09	54.7	0.57	3.50	0.03	-0.104	0.013	-0.030	0.124
RM116-RB bottom	0.10	16.2	9.48	2.54	56.4	0.69	6.35	0.19	-0.152	0.009	-0.024	0.068
RM101-CB bottom	0.09	15.9	9.44	2.83	54.7	0.59	3.16	0.37	-0.170	0.008	-0.054	0.127
RM101-LB bottom	0.09	15.9	9.39	2.59	54.0	0.64	3.16	0.04	-0.141	0.006	-0.045	0.046
RM86-LB bottom	0.10	15.6	9.24	11.70	59.0	0.99	4.63	0.11	-0.145	0.016	-0.031	0.109
RM86-CB bottom	0.10	15.4	9.25	9.94	58.4	0.95	3.67	0.05	-0.214	0.016	-0.058	0.074
RM86-RB bottom												
RM71-CB bottom	0.13	17.5	9.03	1.59	89.1	0.84	43.61	0.45	-0.685	0.025	-0.016	0.037
RM71-LB bottom	0.13	17.8	9.36	1.47	89.1	0.75	56.05	1.71	-0.482	0.017	-0.009	0.047
minimum =	0.09	15.4	9.03	0.94	53.5	0.45	1.73	0.01	-0.685		-0.089	
maximum =	0.13	17.8	9.78	11.70	89.2	0.99	57.77	2.67	-0.008		-0.003	
average =	0.10	16.5	9.47	3.63	61.6	0.66	10.61	0.27	-0.183		-0.032	
std. error =	0.00	0.2	0.04	0.68	2.6	0.03	3.64	0.13	0.039		0.006	

Table 2. Data Summary for Delaware Bay (16 July 2019). Respiration numbers in red are positive values at two upper river stations that were anomalous and not included in the statistics or subsequent data analyses.

			mg O$_2$ L^{-1}	µM			Chla, mg m^{-3}		g O$_2$ m^{-3} d^{-1}		g O$_2$ (mg Chla)$^{-1}$ d^{-1}	
Station	Salinity	Temp °C	DO	NH$_4$	NO$_3$	PO$_4$	ave	se	respiration	se	R^B	se
RM131-LS top	0.13	25.9	7.80	5.19	105.0	2.09	1.91	0.01	1.101	0.066	0.577	0.060
RM131-CS top	0.13	25.6	7.91	2.15	97.2	1.51	1.71	0.02	0.956	0.225	0.561	0.235
RM131-RS top	0.13	25.8	8.00	3.15	96.3	1.63	1.83	0.02	0.281	0.201	0.154	0.713
RM116-LS top	0.10	25.9	6.20	5.19	73.7	2.02	2.90	0.07	1.347	0.304	0.464	0.227
RM116-CS top	0.10	26.0	6.40	5.99	72.5	1.81	1.98	0.15	-0.182	0.193	-0.092	1.061
RM116-RS top	0.10	26.0	6.88	6.12	74.7	1.96	2.15	0.15	-0.259	0.193	-0.121	0.750
RM101-CS top	0.10	26.7	6.82	0.76	77.5	1.35	8.91	0.40	-0.500	0.029	-0.056	0.073
RM101-LS top	0.10	26.8	7.01	0.69	77.6	1.37	9.93	0.69	-0.438	0.076	-0.044	0.187
RM86-LS top	0.12	27.3	7.54	0.69	111.0	1.23	9.04	0.02	-0.554	0.025	-0.061	0.046
RM86-CS top	0.12	27.3	7.40	0.76	112.0	1.14	10.15	0.44	-0.523	0.017	-0.052	0.054
RM86-RS top	0.12	27.0	6.31	0.89	117.0	1.37	8.81	0.48	-0.768	0.333	-0.087	0.437
RM71-CS top	0.17	27.6	6.14	0.75	122.0	1.56	6.02	0.21	-0.237	0.095	-0.039	0.404
RM71-LS top	0.20	27.9	6.54	0.74	118.0	0.89	7.56	0.00	-0.178	0.023	-0.024	0.127
RM131-LB bottom	0.13	25.6	7.92	2.66	104.0	0.76	2.24	0.12	-0.248	0.089	-0.111	0.363
RM131-CB bottom	0.13	25.6	7.87	1.34	98.8	0.77	1.62	0.11	-0.159	0.028	-0.099	0.189
RM131-RB bottom	0.13	25.6	7.90	2.08	96.4	0.94	1.49	0.04	-0.152	0.024	-0.102	0.159
RM116-LB bottom	0.10	25.9	5.43	5.51	72.2	0.98	3.74	0.24	-0.082	0.048	-0.022	0.584
RM116-CB bottom	0.10	25.8	5.47	5.83	72.9	1.06	3.25	0.14	-0.061	0.008	-0.019	0.137
RM116-RB bottom	0.10	25.9	5.61	5.85	73.9	1.06	2.75	0.07	-0.047	0.124	-0.017	2.655
RM101-CB bottom	0.10	26.4	5.58	1.35	82.1	0.98	12.53	0.23	-0.255	0.038	-0.020	0.151
RM101-LB bottom	0.11	26.5	5.82	0.74	80.4	1.14	14.05	0.38	-0.127	0.047	-0.009	0.370
RM86-LB bottom	0.12	27.1	7.34	0.66	112.0	0.99	25.56	0.27	-0.735	0.034	-0.029	0.047
RM86-CB bottom	0.12	26.8	5.96	0.72	116.0	1.23	24.06	0.93	-0.368	0.110	-0.015	0.302
RM86-RB bottom	0.12	26.9	5.58	0.76	118.0	1.28	11.36	0.44	-0.649	0.098	-0.057	0.156
RM71-CB bottom	0.19	27.3	5.48	0.69	122.0	1.62	10.64	0.04	-0.273	0.044	-0.026	0.162
RM71-LB bottom	0.21	27.5	5.73	0.66	119.0	1.58	10.35	0.15	-0.302	0.085	-0.029	0.282
minimum =	0.10	25.6	5.43	0.66	72.2	0.76	1.49	0.00	-0.768		-0.121	
maximum =	0.21	27.9	8.00	6.12	122.0	2.09	25.56	0.93	-0.047		-0.009	
average =	0.13	26.5	6.64	2.38	97.0	1.32	7.56	0.22	-0.322		-0.051	
std. error =	0.01	0.1	0.18	0.42	3.7	0.07	1.27	0.05	0.046		0.008	

Table 3A. Primary Production Parameters: May 2019. Abbreviations: r^2 = coefficient of determination, p = probability due to chance, α = initial slope of light-dependent primary production, $α^b$ = α normalized to chlorophyll a, P_m = maximum rate of primary production, P_m^b = P_m normalized to chlorophyll a, k = water column light extinction coefficient, and Prim. Prod. = primary productivity (integrated rate of C fixation in the water column). Only two of the incubations exhibited saturated uptake of CO_2, enabling estimation of P_m. Station RM86-RS was not sampled in May 2019. Production data for stations RM116-LS and RM101-LS were not well fit by the hyperbolic tangent function, and α or P_m parameters were estimated.

Sample	r^2	regression p	gC m⁻³ (E m⁻²)⁻¹ α	p(α)	gC (E m⁻²)⁻¹ (mg chla)⁻¹ $α^b$	gC m⁻³ d⁻¹ P_m	p(P_m)	gC (mg chla)⁻¹ d⁻¹ P_m^b	ext. coef. k, m⁻¹	gC m⁻² d⁻¹ Prim. Prod.
RM131-LS	0.91	<0.05	0.0017 ± 0.0004	<0.05	0.00062	NA	--	--	0.96	0.081
RM131-CS	0.99	<0.01	0.0019 ± 0.0001	<0.01	0.00103	NA	--	--	1.51	0.028
RM131-RS	0.99	0.07	0.0017 ± 0.0002	0.07	0.00083	NA	--	--	1.21	0.057
RM116-LS	--	--	0.0017	--	0.00067	NA	--	--	1.31	0.046
RM116-CS	0.98	0.10	0.0020 ± 0.0003	0.10	0.00094	NA	--	--	1.31	0.065
RM116-RS	0.97	<0.05	0.0025 ± 0.0003	<0.05	0.00105	NA	--	--	1.06	0.113
RM101-LS	--	--	0.0077	--	0.00313	0.0774 ± 0.0012	<0.01	0.0113	1.13	0.145
RM101-CS	0.86	0.07	0.0030 ± 0.0009	0.07	0.00121	NA	--	--	1.32	0.142
RM86-LS	0.92	<0.01	0.0057 ± 0.0009	<0.01	0.00135	NA	--	--	1.72	0.219
RM86-CS	0.90	0.05	0.0063 ± 0.0015	0.05	0.00191	NA	--	--	0.68	0.562
RM86-RS	--	--	--	--	--	--	--	--	--	--
RM71-CS	0.98	<0.01	0.0154 ± 0.0017	<0.01	0.00040	NA	--	--	1.88	0.588
RM71-LS	0.98	<0.01	0.0335 ± 0.0034	<0.01	0.00058	0.655 ± 0.055	<0.01	0.0317	2.41	0.534
minimum =			0.0035		0.00040	0.077		0.011	0.680	0.028
maximum =			0.2080		0.00313	0.655		0.032	2.410	0.588
average =			0.0348		0.00114	0.366		0.021	1.375	0.215
std. error =			0.0167		0.00022	0.289		0.010	0.132	0.062

	Table 3B. Primary Production Parameters: July 2019. Abbreviations: r^2 = coefficient of determination, p = probability due to chance, α = initial slope of light-dependent primary production, α^b = α normalized to chlorophyll a, P_m = maximum rate of primary production, P_m^b = Pm normalized to chlorophyll a, k = water column light extinction coefficient, and P = primary productivity (integrated rate of C fixation in the water column).									

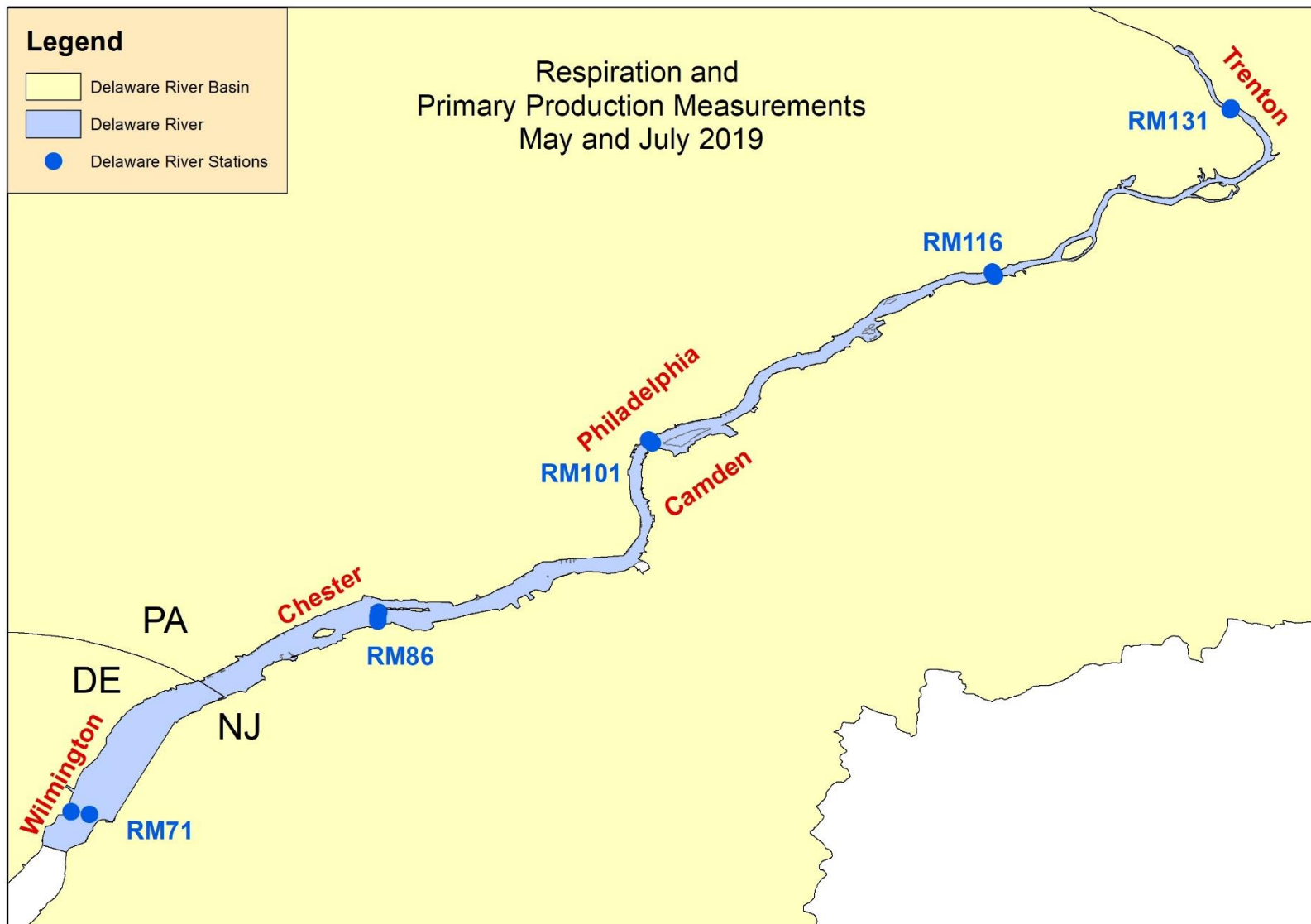| Sample	r^2	regression p	$gC\ m^{-3}\ (E\ m^{-2})^{-1}$ α	p(α)	$gC\ (E\ m^{-2})^{-1}\ (mg\ chla)^{-1}$ α^b	$gC\ m^{-3}\ d^{-1}$ P_m	$p(P_m)$	$gC\ (mg\ chla)^{-1}\ d^{-1}$ P_m^b	ext. coef. k, m^{-1}	$gC\ m^{-2}\ d^{-1}$ P
RM131-LS	0.98	<0.01	0.0106 ± 0.0009	<0.01	0.0055	indeterminate	--	--	2.41	0.249
RM131-CS	0.98	<0.01	0.0047 ± 0.0004	<0.01	0.0028	indeterminate	--	--	2.27	0.148
RM131-RS	0.99	<0.01	0.0096 ± 0.0007	<0.01	0.0053	indeterminate	--	--	1.84	0.303
RM116-LS	0.99	<0.01	0.0088 ± 0.0005	<0.01	0.0030	indeterminate	--	--	2.07	0.226
RM116-CS	0.91	<0.05	0.0097 ± 0.0017	<0.05	0.0049	indeterminate	--	--	1.70	0.308
RM116-RS	0.99	<0.01	0.0079 ± 0.0004	<0.01	0.0037	indeterminate	--	--	2.08	0.287
RM101-LS	0.99	<0.01	0.0361 ± 0.0017	<0.01	0.0041	0.920 ± 0.028	<0.01	0.1033	1.46	0.690
RM101-CS	0.99	<0.01	0.0340 ± 0.0026	<0.01	0.0034	0.613 ± 0.030	<0.01	0.0618	2.37	0.404
RM86-LS	0.99	<0.01	0.0338 ± 0.0027	<0.01	0.0037	0.728 ± 0.053	<0.01	0.0480	3.00	0.497
RM86-CS	0.94	<0.01	0.0384 ± 0.0074	<0.05	0.0038	0.667 ± 0.099	<0.01	0.0668	2.98	0.528
RM86-RS	0.99	<0.01	0.0304 ± 0.0018	<0.01	0.0035	0.736 ± 0.043	<0.01	0.0614	2.87	0.507
RM71-CS	0.99	<0.01	0.0175 ± 0.0014	<0.01	0.0029	0.543 ± 0.051	<0.01	0.0447	3.25	0.290
RM71-LS	0.97	<0.01	0.0181 ± 0.0024	<0.01	0.0024	0.664 ± 0.018	<0.05	0.0577	2.74	0.385
minimum =			0.0079		0.0024	0.543		0.0447	1.46	0.148
maximum =			0.0384		0.0053	0.920		0.1033	3.25	0.690
average =			0.0200		0.0038	0.696		0.0634	2.39	0.371
std. error =			0.0035		0.0003	0.045		0.0073	0.15	0.042

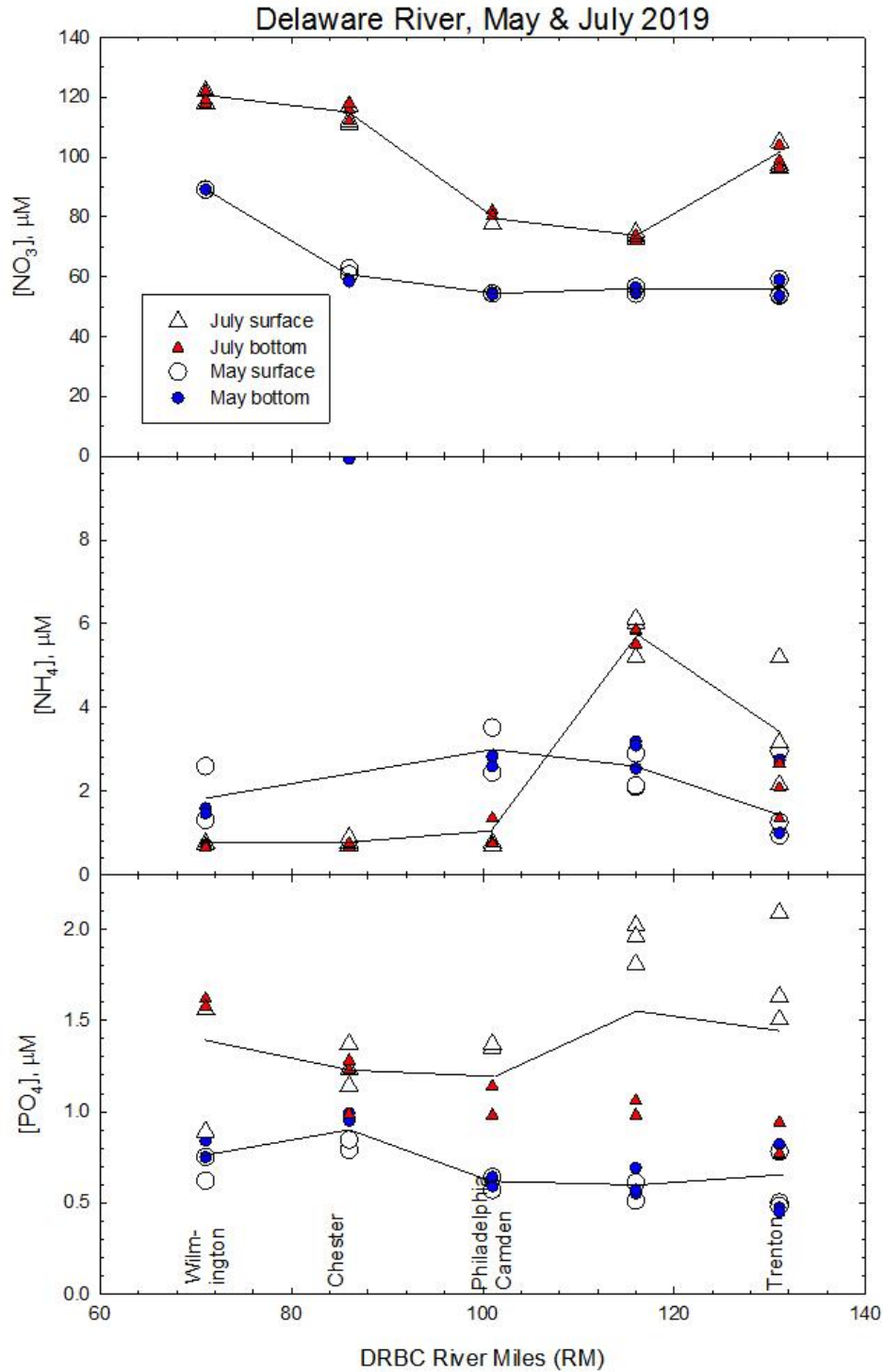**Figure 1**. Map of sampling locations in the Delaware River at River Mile (RM) 71 to 131 in May and July 2019.

Figure 2. Distribution of nitrate (NO_3), ammonium (NH_4), and phosphate (PO_4) in surface and bottom waters of the Delaware River. There were no consistent significant differences between surface and bottom concentrations. Symbols differ in size only to show overlapping values.
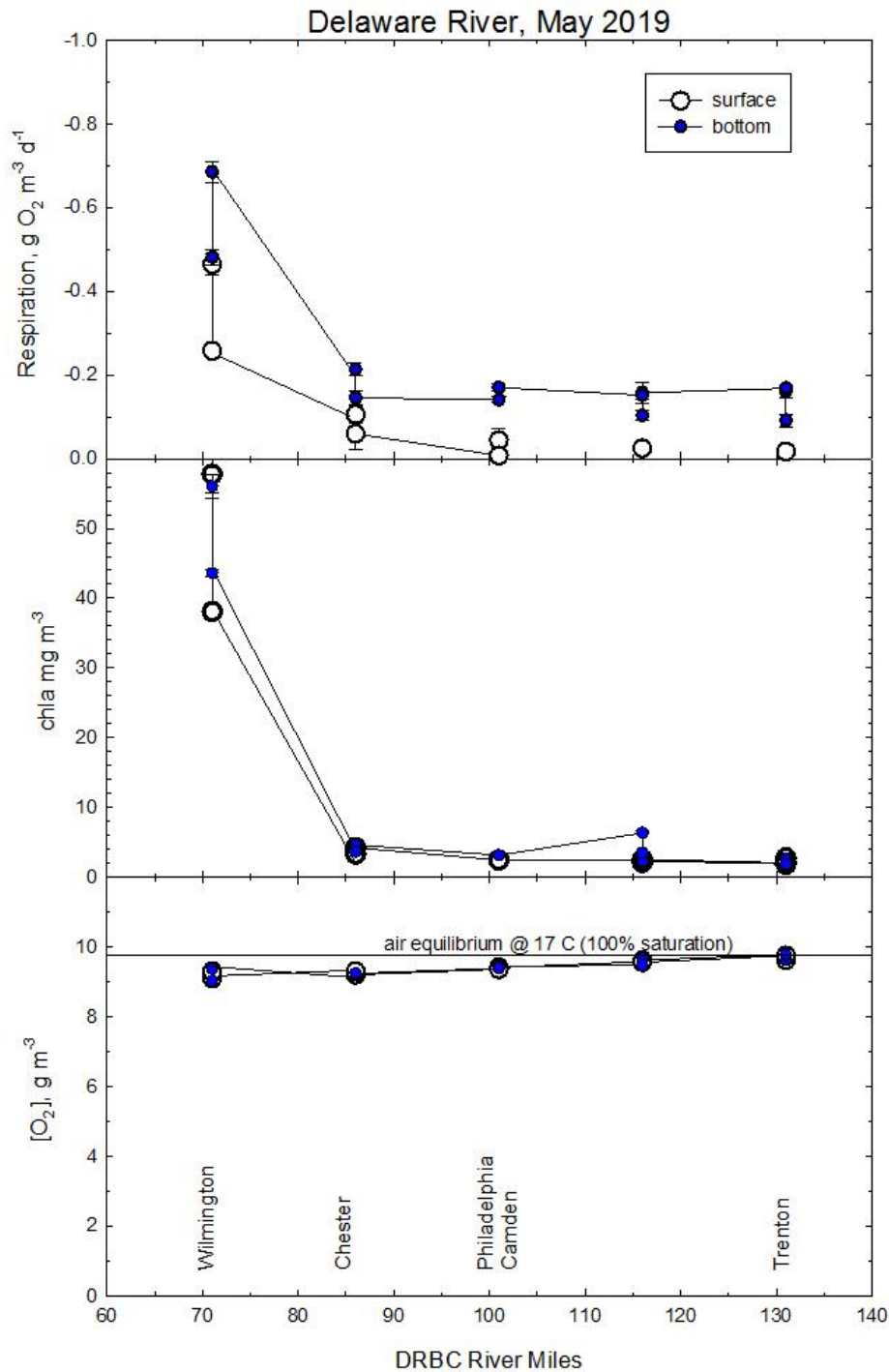
Figure 3A. Respiration, chlorophyll *a*, and dissolved O$_2$ in the Delaware River in May 2019. Respiration and chlorophyll a in the lower river was elevated compared to the upper river, and oxygen was slightly undersaturated in this area as well. Air equilibrium for O$_2$ was calculated from temperature and salinity using Colt (1984).
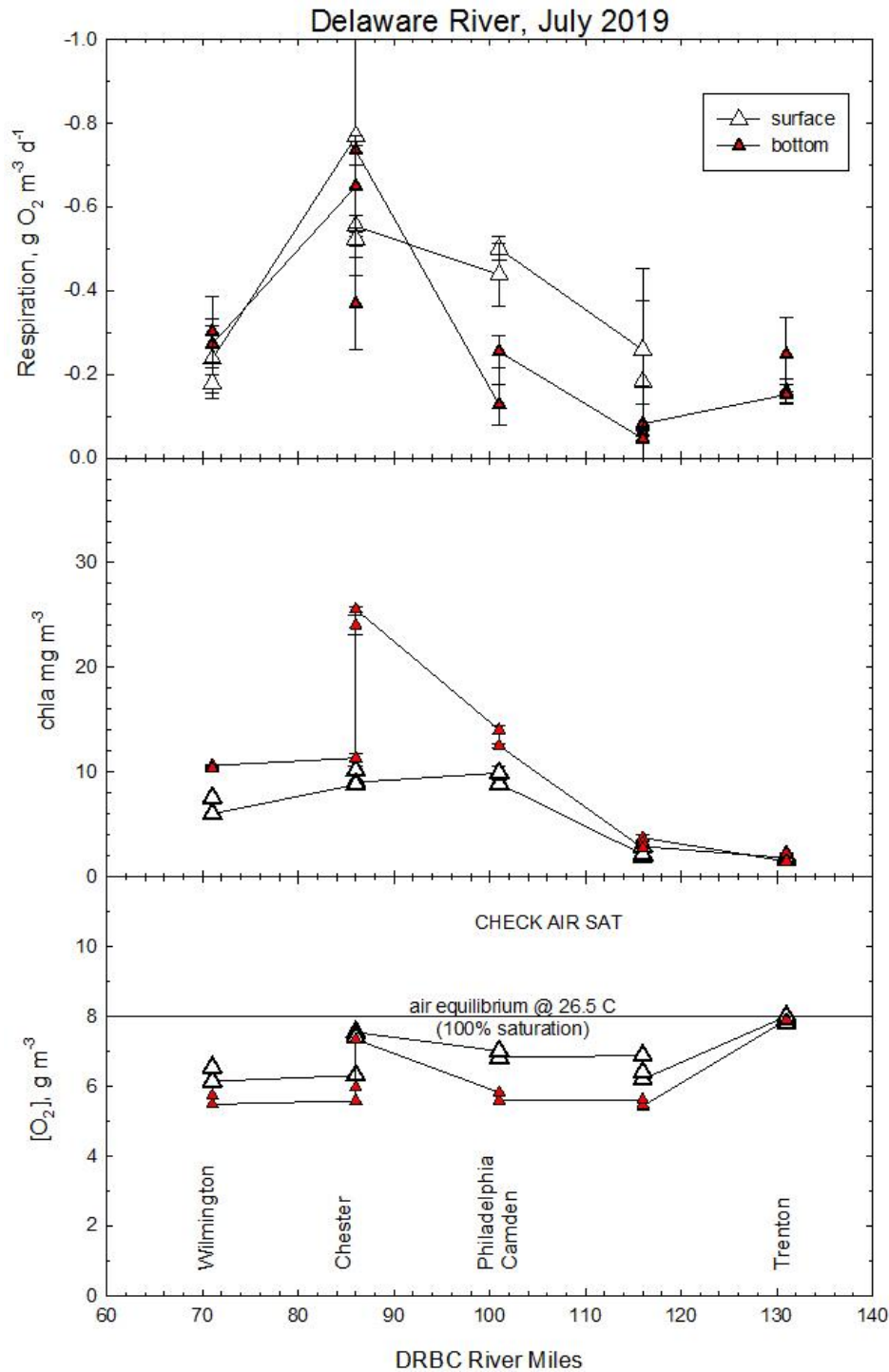
Figure 3B. Respiration, chlorophyll a, and dissolved O_2 in the Delaware River in July 2019. Chlorophyll *a* values were slightly lower than those in May, but respiration there was similar or slightly higher. There was an oxygen deficit in July 2019 in both surface and bottom waters similar to observations in July 2018. Air equilibrium for O_2 was calculated from temperature and salinity using Colt (1984).
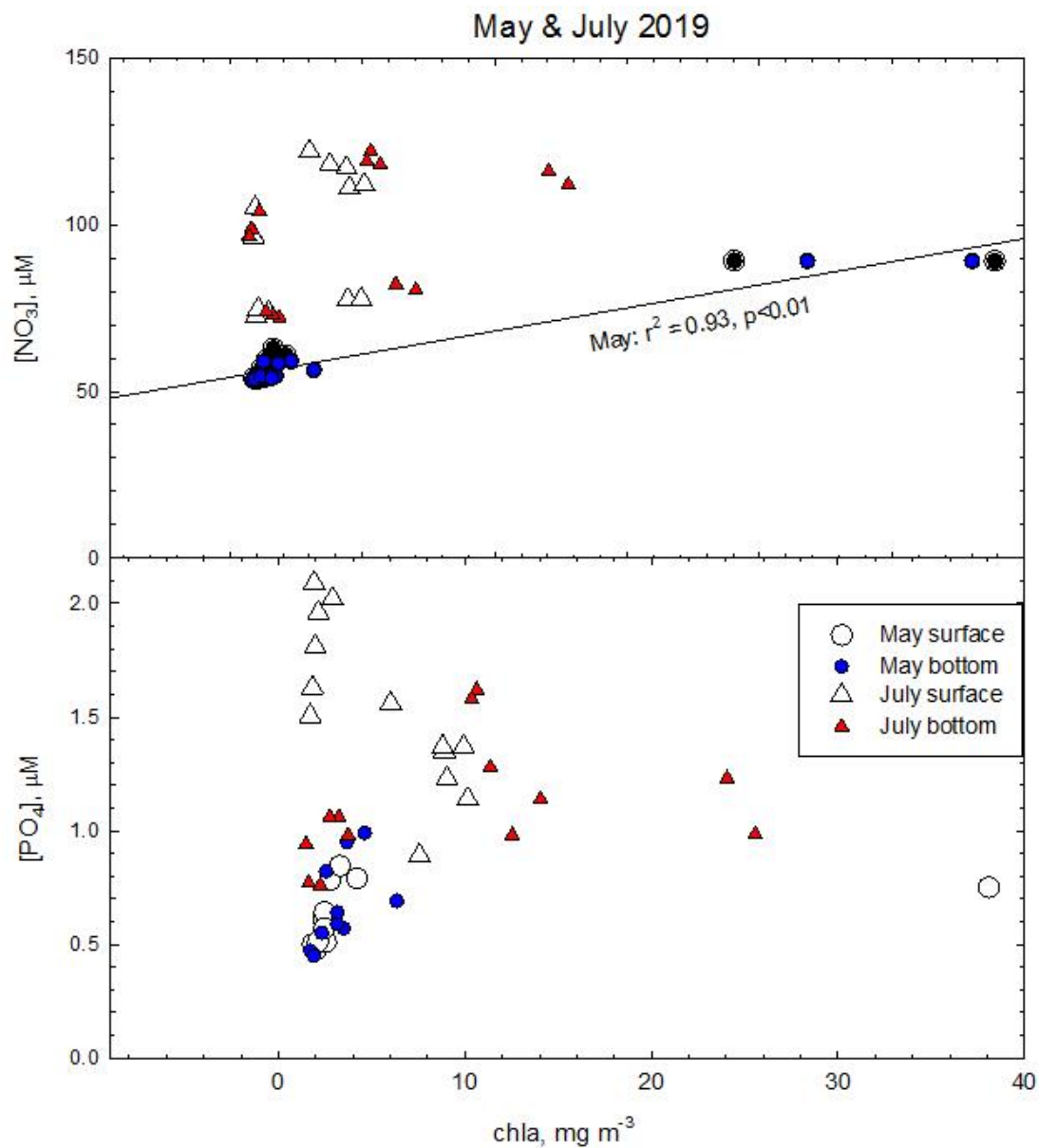
Figure 4. Relationships of chlorophyll *a* with nitrate (NO_3) and phosphate (PO_4) concentrations in the two time periods. Phosphate was independent of chlorophyll *a* concentrations, but in May there was a positive linear relationship with nitrate.

Delaware River, May 2019

surf resp = 0.0259 − 0.00821 * bot chla, r^2 = 0.81, p<0.01

bot resp = −0.126 − 0.00874 * bot chla, r^2 = 0.82, p<0.01

○ surface
● bottom

RM 71-CS, LS

Delaware River, July 2019

resp = 0.180 − 0.0411 * chla
r^2 = 0.26, p<0.01

△ surface
▲ bottom
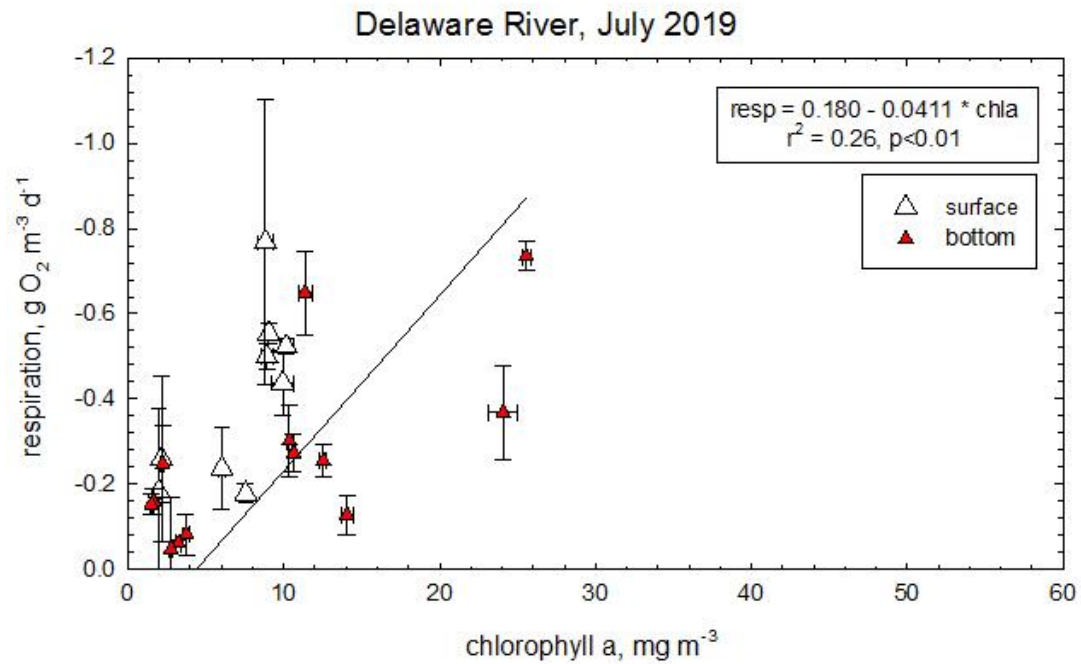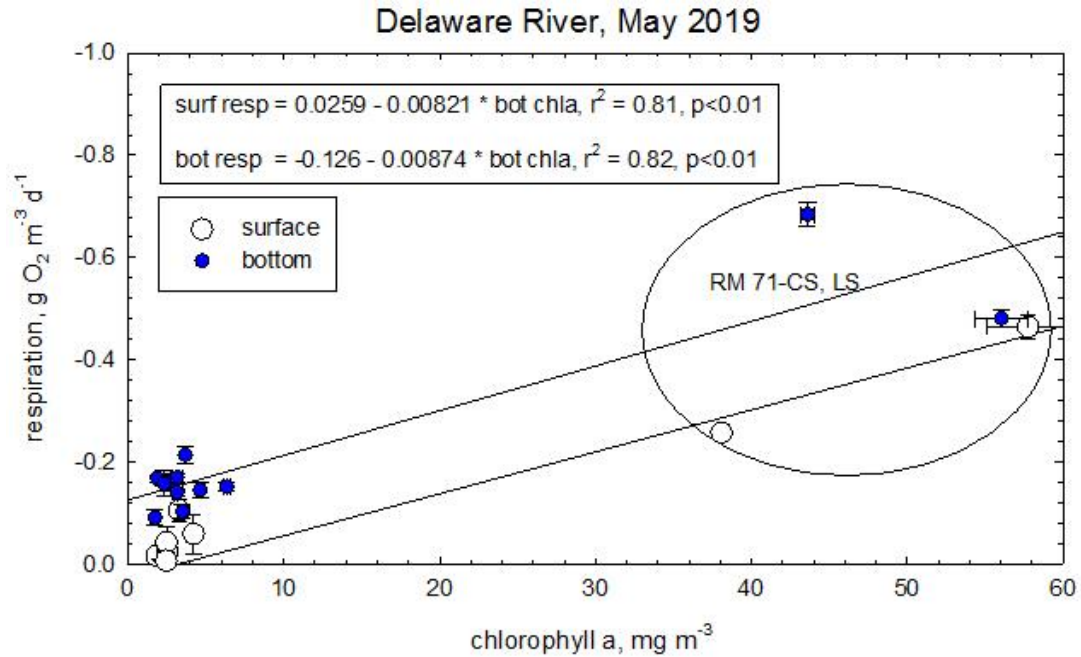
Figure 5. Respiration as a function of chlorophyll *a* in the Delaware River for May and July 2019. Respiration was positively correlated with river chlorophyll *a* in both months, but respiration in bottom waters in May 2018 was significantly elevated compared to surface waters. The bloom conditions at station RM71 resulted in high respiration rates in May equivalent to those observed in July at much warmer temperatures.

31
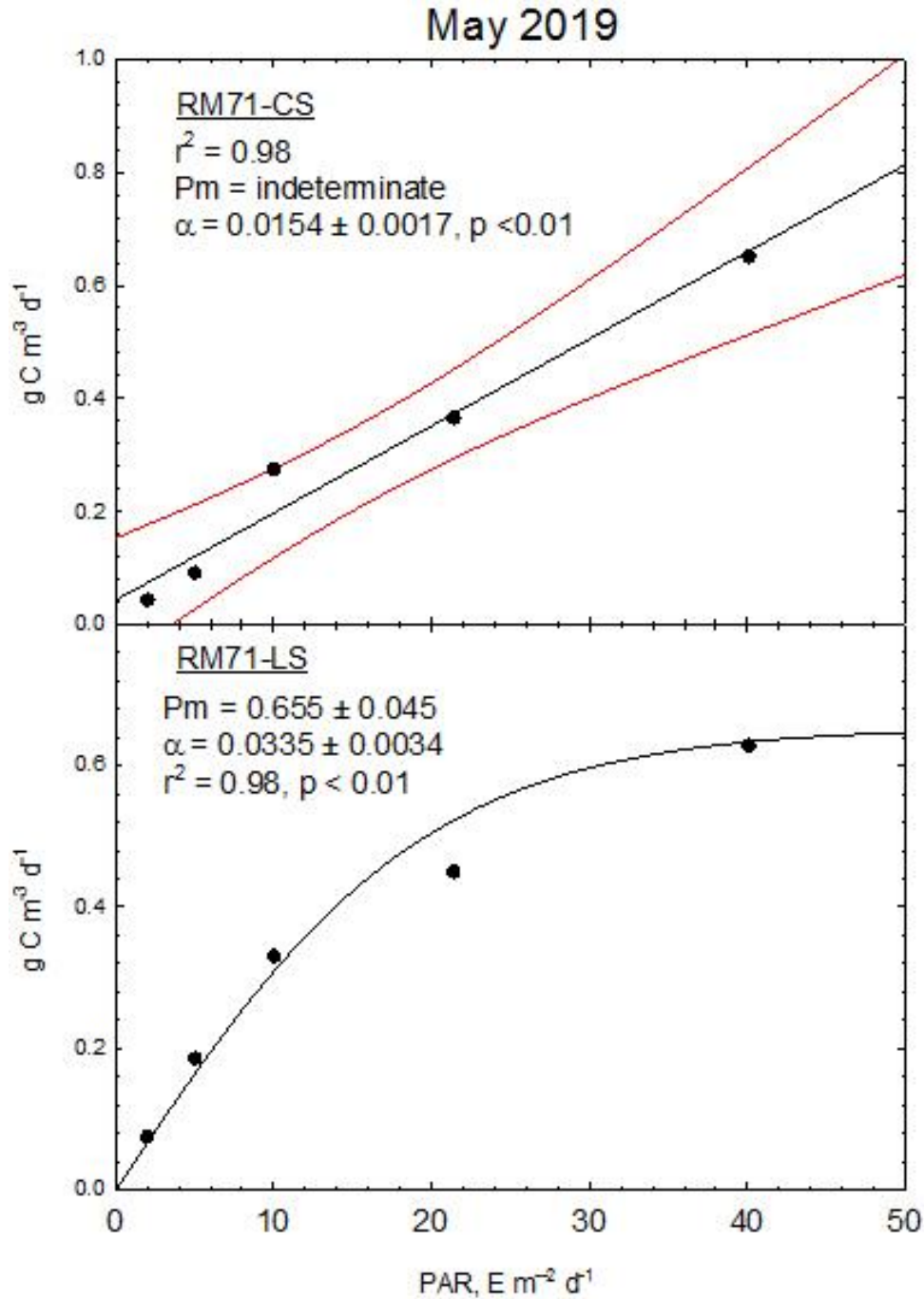
Figure 6A. Two examples of the hyperbolic tangent fit of eq. 7 to production vs PAR data. The top panel is essentially a linear response to PAR (Sharp type 1). The initial linear response to PAR, α, was estimated, but P_m, the maximum rate of primary production, could not be determined in this example. The bottom panel is an example where primary production was approaching light saturation at PAR = 40 E m^{-2} d^{-1} (Sharp type 2), and both α and P_m were estimated. There were no examples of Sharp type 3 (light inhibition) in this dataset. Red curved lines are 95% confidence intervals.

Primary Production, g C m^{-3} d^{-1}
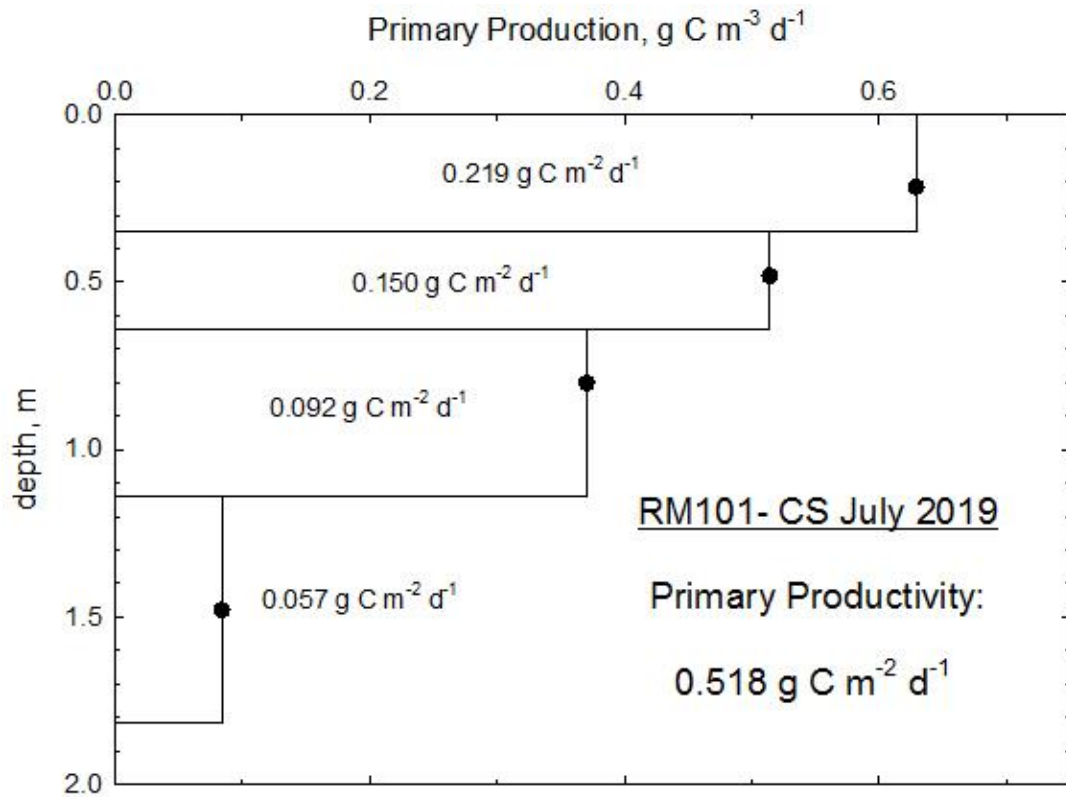
Figure 6B. Example of depth integration to obtain integrated primary productivity (P, g C m^{-2} d^{-1}) at each station from the individual measurements of primary production (P$_z$, g C m^{-3} d^{-1}) at fixed light depths of 3-60% ambient light. Light depths (I$_z$/I$_0$) were converted to water column depths using the measured extinction coefficient (k, m^{-1}) at each station (eq. 8), and primary productivity in each depth interval (ΔZ) was computed as P$_z$ * ΔZ and summed vertically for the total station primary productivity (eq. 9).

Delaware River 2019

P_m , gC m^{-3} d^{-1}

1.0

0.8

0.6

0.4

0.2

0.0

0.00   0.01   0.02   0.03   0.04   0.05

α, gC m^{-3} (E m^{-2})$^{-1}$

- May
- July

$P_m = 1.36 * \tanh(0.0433 * \alpha)$
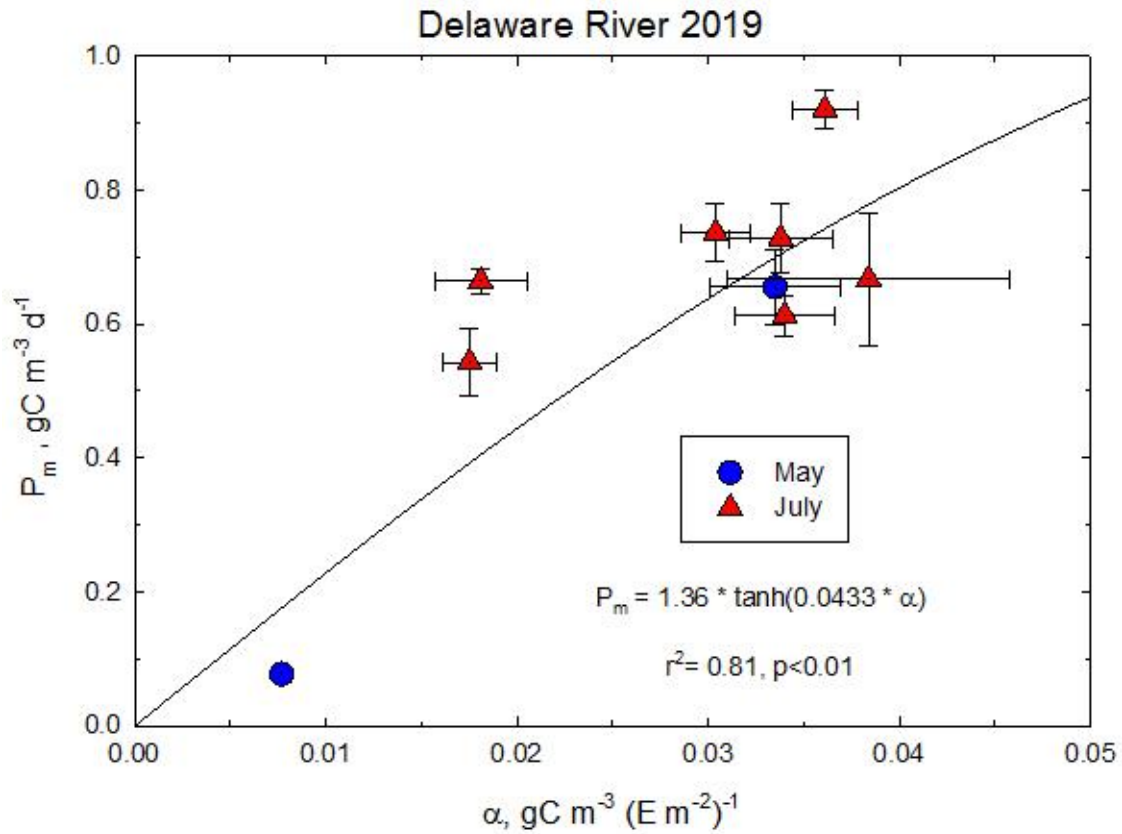
$r^2 = 0.81$, p<0.01

Figure 7. Relationship between the two photosynthetic parameters P_m (light-saturated primary production) and α (light-dependent primary production) in May and July 2019 in the Delaware River stations.
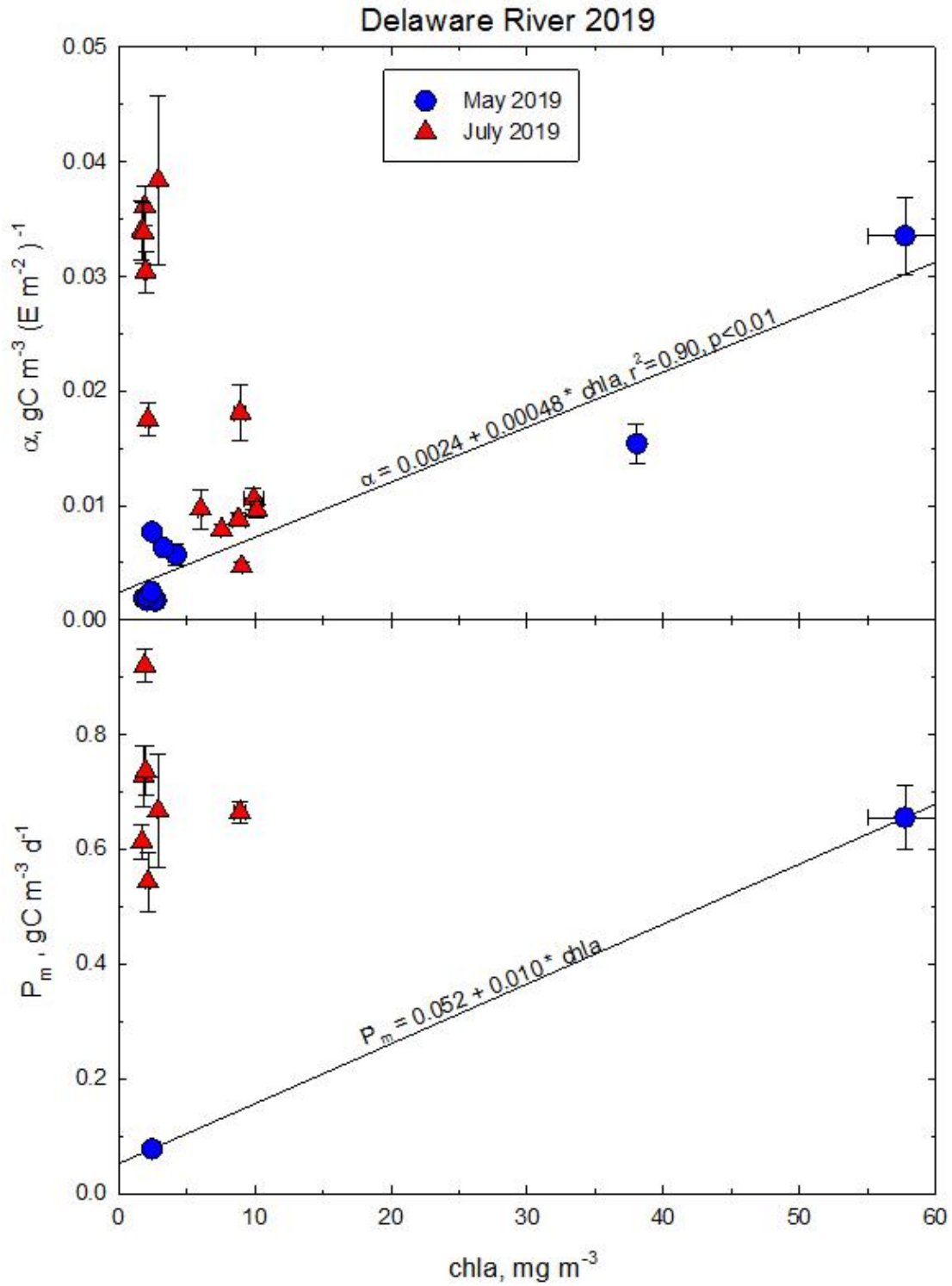
Figure 8. Relationships between the photosynthetic parameters α and P_m to chlorophyll *a* (chla) in May and July 2019 at river mile stations (RM) in the Delaware River. There was a clearly defined relationship between algal biomass (chla) and the parameters in May, but not in July.
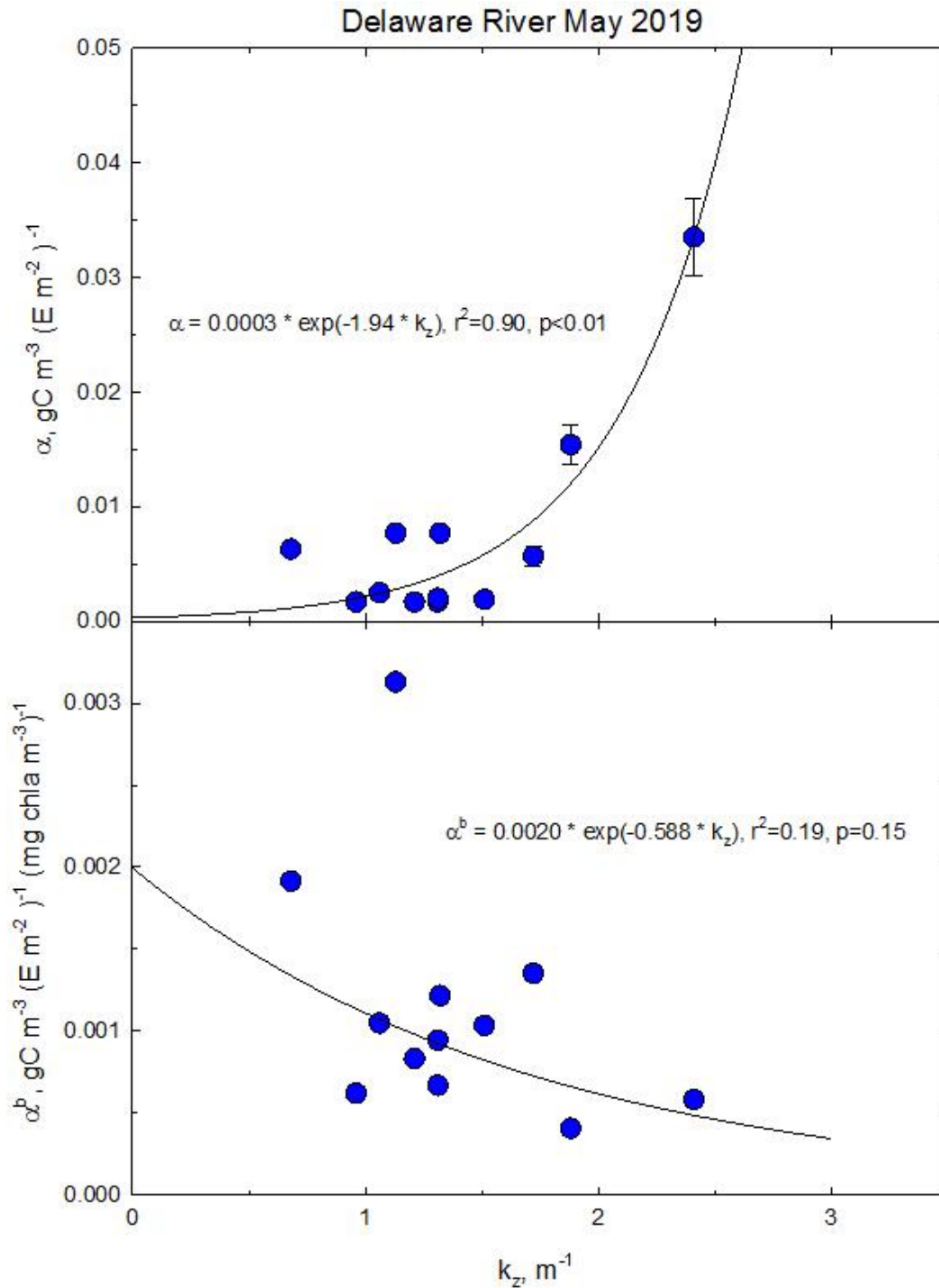
Figure 9A. The relationship of the light-dependent photosynthetic parameters α and α^b to the water column extinction coefficient for PAR (k_z) in May 2019. There was a significant exponential increase in α as k_z increased, but there were no significant linear, negative exponential, or negative hyperbolic relationships of α^b with k_z in the lower panel. It is clear that there was a negative relationship, and the best fit was exponential, which is shown.
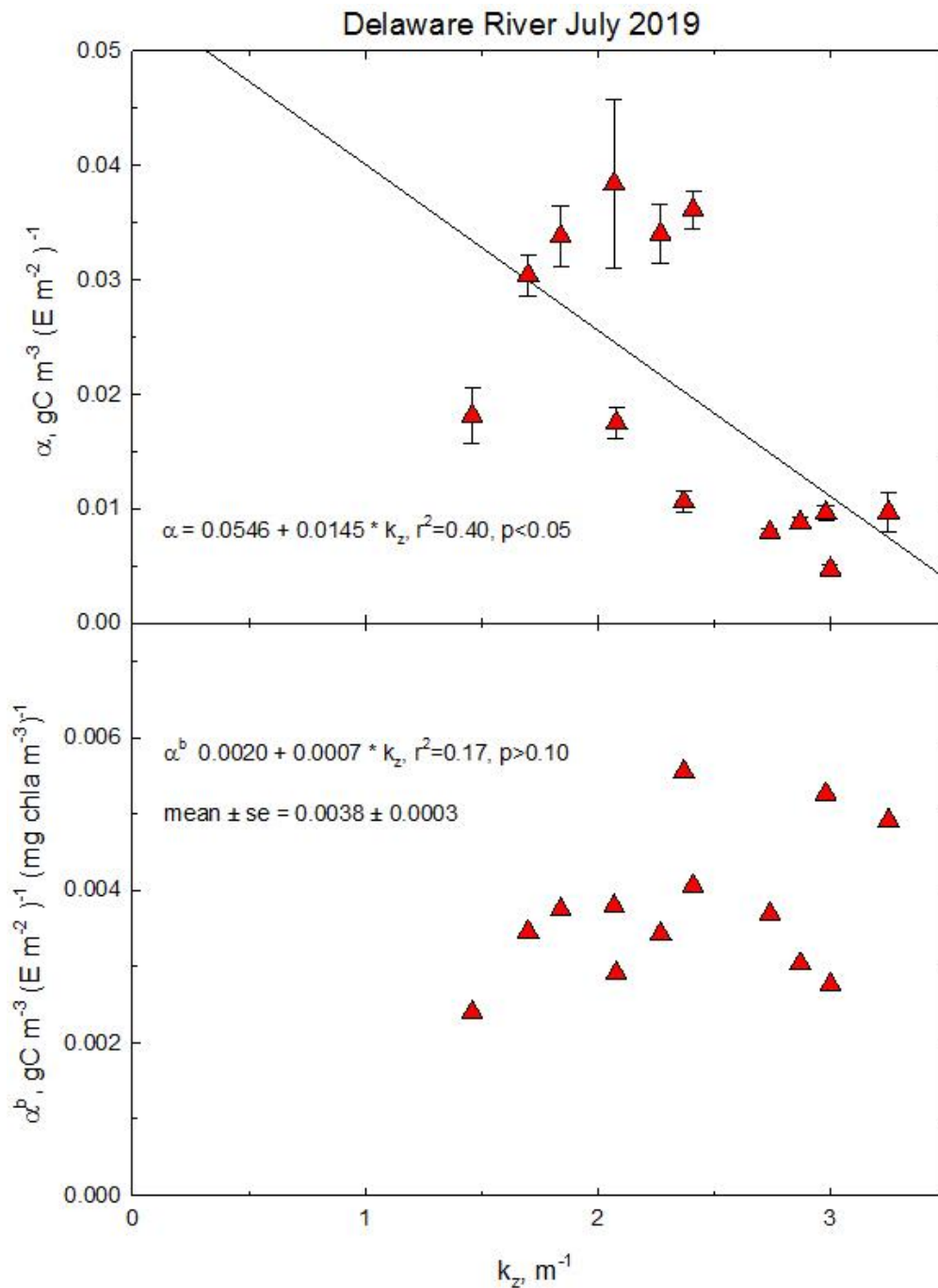
Delaware River July 2019

$\alpha = 0.0546 + 0.0145 * k_z$, $r^2 = 0.40$, $p < 0.05$

$\alpha^b = 0.0020 + 0.0007 * k_z$, $r^2 = 0.17$, $p > 0.10$

mean $\pm$ se $= 0.0038 \pm 0.0003$

Figure 9B. The relationship of the light-dependent photosynthetic parameters α and α^b to the water column extinction coefficient for PAR (k_z) in July 2019. There was a significant linear decrease in α as k_z increased in the upper panel, but in the lower panel there were no significant relationship of α^b with k_z in July 2019.
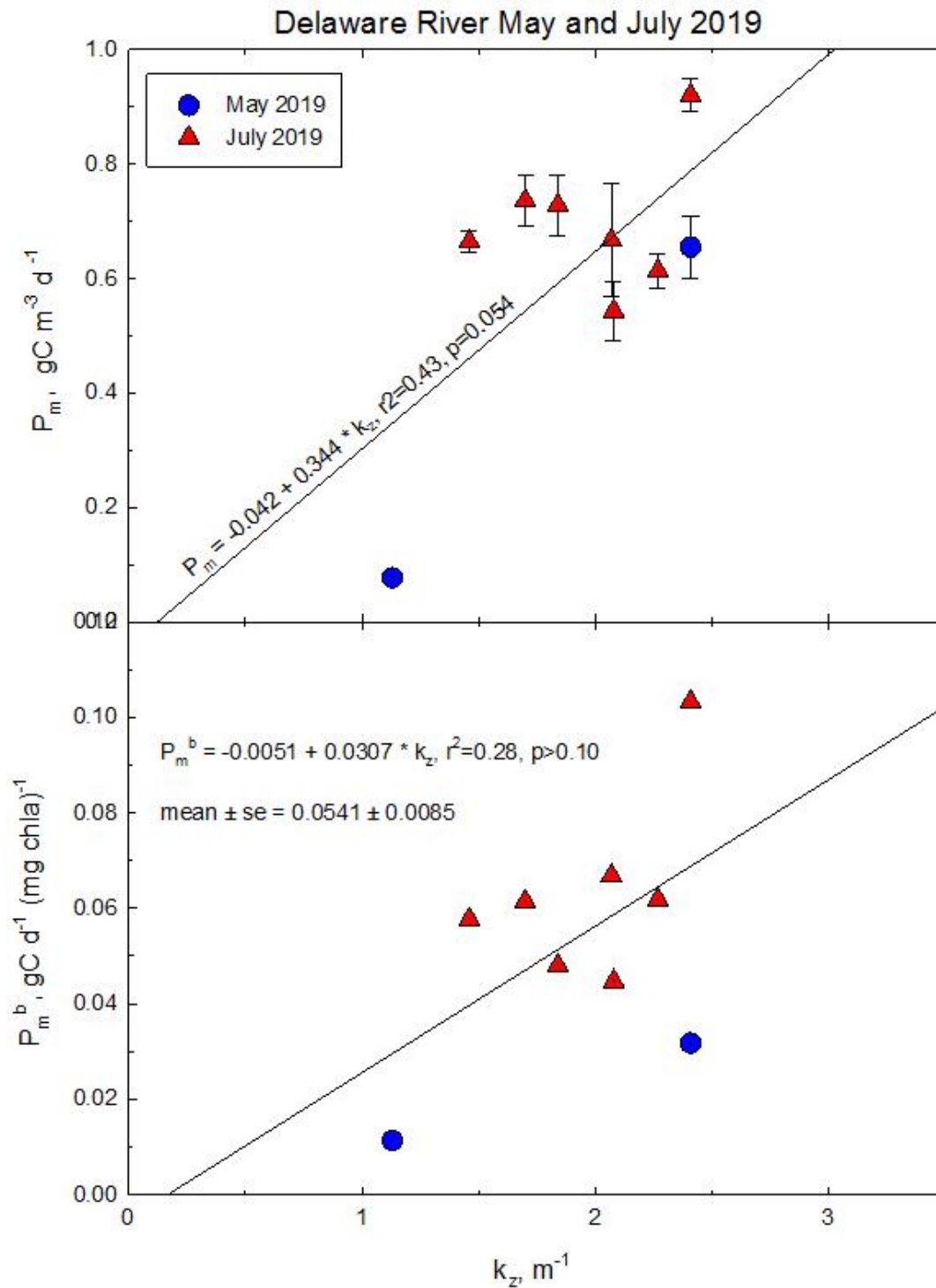
Figure 9C. The relationship of the light-saturated photosynthetic parameters P_m and P_m^b to the water column extinction coefficient for PAR (k_z) for both May and July 2019. There was a marginally significant, linear relationship between P_m and k_z (upper panel), and an inverse relationship between P_m^b and k_z (lower panel) which was not significant ($p > 0.10$).
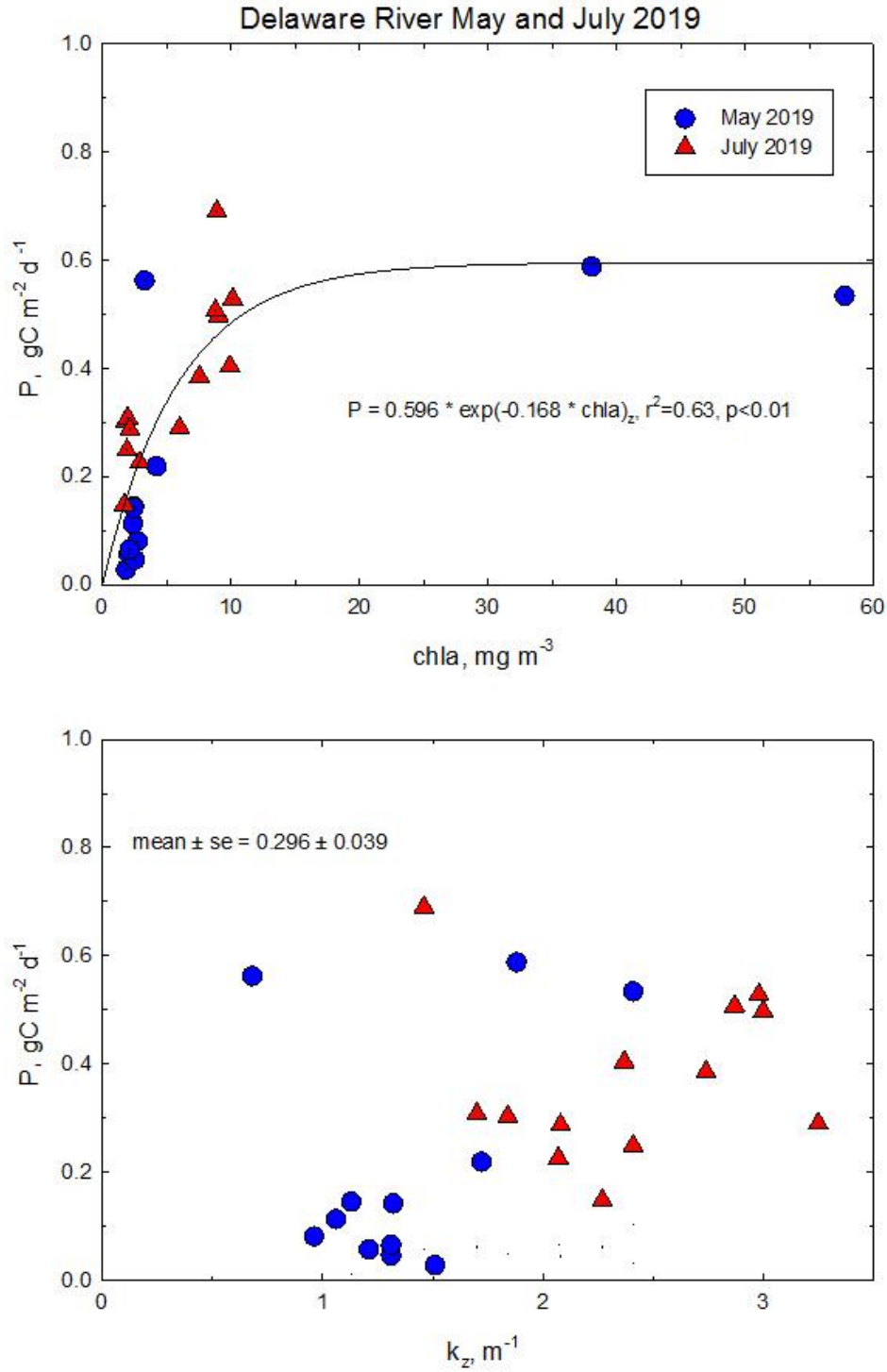
Figure 10. Integrated primary (P) in the water column as a function of surface chlorophyll *a* for May and July 2019 (upper panel), and the relationship of P to the water column extinction coefficient (k_z) for May and July (lower panel). In this dataset, P is an exponential function of surface chlorophyll a, but unrelated to the water column extinction coefficient.